Received: 29 June 2016 | Accepted: 23 August 2016

DOI: 10.1111/cpr.12296

ORIGINAL ARTICLE

WILEY Cell Proliferation

Gold nanoparticle–conjugated quercetin inhibits epithelial–mesenchymal transition, angiogenesis and invasiveness *via* EGFR/VEGFR-2-mediated pathway in breast cancer

S. Balakrishnan[1] | F. A. Bhat[1] | P. Raja Singh[1] | S. Mukherjee[2,3] | P. Elumalai[1] | S. Das[2,3] | C. R. Patra[2,3] | J. Arunakaran[1]

[1]Department of Endocrinology, Dr. ALM Post Graduate Institute of Basic Medical Sciences, University of Madras, Taramani Campus, Chennai 600113, India

[2]Biomaterials Group, CSIR-Indian Institute of Chemical Technology, Tarnaka, Hyderabad 500007, Telangana State, India

[3]Academy of Scientific and Innovative Research (AcSIR), Training and Development Complex, CSIR Campus, Taramani, Chennai 600 113, India

Correspondence
J. Arunakaran, Department of Endocrinology, Dr. ALM Post Graduate Institute of Basic Medical Sciences, University of Madras, Taramani Campus, Chennai, India.
Email: j_arunakaran@hotmail.com

Correction added on 28th September 2016, after first online publication: The Results section in the article abstract was previously incorrect and is now corrected in this version.

Abstract

Objectives: Epidermal growth factor plays a critical role in breast malignancies by enhancing cell proliferation, invasion, angiogenesis and metastasis. Epithelial–mesenchymal transition (EMT) is a crucial process by which epithelial cells lose polarity and acquire migratory mesenchymal properties. Gold nanoparticles are an efficient drug delivery vehicle for carrying chemotherapeutic agents to target cancer cells and quercetin is an anti-oxidative flavonoid known with potent anti-malignant cell activity.

Materials and methods: Cell viability was assessed by MTT assay, and protein expression was examined by Western blotting and immunocytochemistry. Cell invasion was monitored using invasion chambers, and cell migration was analysed by scratch wound-healing assay. In vitro and ex vivo angiogenesis studies were performed by capillary-like tube formation assay and chick embryo angiogenesis assay (CEA). 7,12-dimethylbenz(a) anthracene (DMBA) induced mammary carcinoma in Sprague-Dawley rats.

Results: We observed a significant reduction in protein expression of vimentin, N-cadherin, Snail, Slug, Twist, MMP-2, MMP-9, p-EGFR, VEGFR-2, p-PI3K, Akt and p-GSK3β, and enhanced E-cadherin protein expression in response to AuNPs-Qu-5 treatment. AuNPs-Qu-5 inhibited migration and invasion of MCF-7 and MDA-MB-231 cells compared to free quercetin. AuNPs-Qu-5-treated HUVECs had reduced cell viability and capillary-like tube formation. In vitro and in vivo angiogenesis assays showed that AuNPs-Qu-5 suppressed tube and new blood vessel formation. Treatment with AuNPs-Qu-5 impeded tumour growth in DMBA-induced mammary carcinoma in SD rats compared to treatment with free quercetin.

Conclusion: Our results suggest that AuNPs-Qu-5 inhibited EMT, angiogenesis and metastasis of the breast cancer cells tested by targeting the *EGFR/VEGFR-2* signalling pathway.

1 | INTRODUCTION

Breast carcinoma is the most common type of cancer among women and second leading cause of death around the globe. It is now estimated that 246 660 new cases of invasive breast cancer are expected to be diagnosed in women in the United States.[1] Nearly 90% cancer-related mortality is caused by cancer metastasis.[2] Metastasis is a complex, multistep process whereby tumour cells acquire the characteristics necessary to escape their original environment, survive in the bloodstream, seed and propagate at distant sites. Epithelial–mesenchymal transition (EMT) is recognized as a critical event for metastasis of carcinomas and a key player in promoting metastasis in epithelium-derived cancer cells. These epithelial cells lose the polarity and gain motile mesenchymal properties[3,4] with increased expression

 © 2016 John Wiley & Sons Ltd

of N-cadherin and decreased expression of E-cadherin, thus aiding in invasiveness.[5] E-cadherin is a well-known tumour suppressor, and the "E-cadherin to N-cadherin" switch is routinely used to monitor EMT both during embryonic development and cancer progression.[6]

Strong evidences substantiate that E-cadherin expression is down-regulated in poorly differentiated tumour cells, such as breast cancer,[7] stomach cancer[8] and liver cancer.[9] Transcriptional factors such as Snail, Slug and Twist regulate EMT especially E-cadherin expression.[10] In human breast cancer, Snail and Slug can repress E-cadherin expression in vitro, but Slug expression alone was correlated with E-cadherin down-regulation in vitro.[11] These transcription factors also regulate matrix metalloproteinases (MMPs).[12] MMPs are zinc-dependent proteases that play a definitive role in proteolytic degradation of ECM components and aid in breaching the basement membrane, thus leading to tumour invasion and metastasis.

Epithelial–mesenchymal transition is stimulated by various signals from the tumour microenvironment, which include varieties of growth factors and cytokines. Vascular endothelial growth factor receptor (VEGFR) orchestrated signalling is one of the most important and sophisticated regulatory signalling pathways in human cancer. It exerts stringent control over cell proliferation, differentiation, invasion, migration and interactions with the cellular milieu. VEGFR-2 plays a crucial role in mediating the cell survival and proliferation of endothelial cells.[13] Epidermal growth factor (EGF) can induce EMT in various cancer cell lines.[14–16] EGF–EGFR binding results in dimerization and auto-phosphorylation of the receptor and subsequent recruitment of downstream molecules PI3K/Akt that mediate cell proliferation, invasion and migration.[17] Epidemiological and dietary intervention studies in animals and humans have suggested that bioflavonoids, such as quercetin, play a beneficial role in retarding the progression of carcinogenesis in various cancer.[18,19] Recent studies documented quercetin (Qu) to be a potent anticancer agent that modulates proliferation, survival and differentiation of tumour cells. Bhat et al.[20] reported that quercetin inhibits EGF-induced epithelial-to-mesenchymal transition *via* EGFR/PI3K/Akt pathway in prostate cancer (PC-3) cells. However, the therapeutic effect of Qu is restricted owing to its poor solubility in aqueous solution. On to enhance Qu efficiency, we formulated gold nanoparticle-based drug delivery system for Qu (AuNPs-Qu-5) and used these nanoconjugates against the cancer cells. Recently, researchers have introduced various metal-based nanoparticle innovative inventions for potential therapeutic applications in the field of biomedical research.[21] Among the nanocarriers, gold nanoparticles have drawn more attention in huge area of research.[22]

The study of gold nanoparticle–conjugated quercetin in EMT, migration, invasion, angiogenesis and tumour growth in breast cancer is unexplored yet. Hence, the present investigation was aimed to disclose the molecular mechanisms underlying inhibition of EMT, angiogenesis and metastasis in human breast cancer cell lines (MCF-7 and MDA-MB-231). In this study, we observed that AuNPs-Qu-5 significantly down-regulated the protein expression involved in EMT, angiogenesis, tumour growth and metastasis. Cytotoxicity, wound healing, invasion and tube formation assays showed the effective anti-angiogenesis activity of AuNPs-Qu-5 in vitro in human umbilical vein endothelial cells (HUVECs). The anti-angiogenesis activity was also reproduced ex vivo using chick embryo angiogenesis assay (CEA). Finally, we validated that AuNPs-Qu-5 causes tumour regression in DMBA-induced mammary carcinoma in Sprague-Dawley rats.

2 | MATERIALS AND METHODS

2.1 | Chemicals

Tetrachloroauric (III) acid ($HAuCl_4$, $3H_2O$), quercetin, Dulbecco's modified Eagle medium (DMEM), 4,6-diamidino-2-phenylindole (DAPI) and β-actin (mouse monoclonal antibody) and 7, 12-Dimethylbenz (a) anthracene (DMBA) were purchased from Sigma Aldrich Chemicals Pvt. Ltd. (St. Louis, MO, USA). Polyvinylidene difluoride (PVDF) membrane was purchased from Millipore (Billerica, MA, USA). Foetal bovine serum (FBS) and trypsin EDTA were obtained from Gibco (Invitrogen, Carlsbad, CA, USA). Primary antibodies for VEGFR-2, p-EGFR, p-PI3K, Akt, p-Akt, p-GSK-3β, Snail, Slug, Twist, MMP-2, MMP-9, E-cadherin, N-cadherin and vimentin (mouse monoclonal and rabbit monoclonal) were purchased from Cell Signaling (3 Trask Lane Danvers, MA, USA). Anti-N-cadherin antibody was purchased from Thermo Scientific Pierce (Rockford, IL, USA). Anti-vimentin and anti-E-cadherin antibodies were obtained from Santa Cruz Biotechnology (Santa Cruz, CA, USA). The secondary antibodies horseradish peroxidase (HRP)-conjugated, tetramethylrhodamine (TRITC and Alexa FITC)-conjugated rabbit-anti-mouse immunoglobulin (Ig) G and goat-anti-rabbit IgG were obtained from Genei, Bangalore, India. Other chemicals were obtained from Sisco Research Laboratories (SRL), Pvt. Ltd., Andheri East, India.

2.2 | Synthesis of gold nanoparticles

The synthesis of gold nanoparticles was carried out following the method of Bhattacharya et al.[23] Briefly, 50 mL of $NaBH_4$ (0.1 mg/mL) in water was added very slowly to a mixture of 99 mL of water and 1 mL of 10^{-2} M of $HAuCl_4$ solution in a 250 mL beaker, with continuous stirring. The solution was kept overnight stirring for completion of the reaction.

2.3 | Conjugation of quercetin with gold nanoparticles

In order to prepare nano-conjugated system, the quercetin (5 μg/mL) was conjugated with gold nanoparticles (AuNPs) for 45 minutes with continuous stirring. The resulting AuNP-conjugated quercetin (AuNPs-Qu-5) was purified using ultracentrifugation at 25 024 ***g*** for 40 minutes at 15°C. The intensely red coloured loose pellet of the drug-loaded AuNPs-Qu-5 was used for further characterization and biological experiments.[24]

2.4 | UV-Visible spectroscopy

The absorption of AuNPs, AuNPs-Qu-5 and Qu was typically measured by UV-Vis spectroscopy (JASCO dual-beam spectrophotometer

[Model V-570]) in a quartz cuvette from 800 to 200 nm with a resolution of 1 nm.

2.5 | Preparation of a standard curve for quercetin (Qu) and quantification of Qu in AuNPs-Qu-5 by UV-Visible spectroscopy

UV-Visible spectroscopy was used to make a standard curve of quercetin (5–25 μg/mL in AuNPs supernatant) by plotting the absorbance of Qu (λ_{max} ~ 379.5 nm) at their respective concentrations (μg/mL). The amount of unconjugated Qu in the supernatant of AuNPs-Qu-5 and the per cent of Qu attachment in AuNPs-Qu-5 were calculated using the standard curve and the absorbance of the AuNPs-Qu-5 supernatant.

2.6 | DLS (dynamic light scattering) study

Dynamic light scattering is used for measuring the size of the nanoparticles. The average particle size distribution of AuNPs and AuNPs-Qu-5 was recorded using a Zetasizer Ver. 6.20, Malvern Instruments Ltd. (Malvern, Worcestershire, UK) by taking 1 mL of each nanoparticles solution in quartz cuvette for analysis.

2.7 | FT-IR spectroscopy

FT-IR analysis is essential for the identification of functional groups present in the compound. The intensely red coloured and deep reddish black coloured pellet of AuNPs and AuNPs-Qu-5, respectively, were lyophilized to make them powder. Both the nanoparticles were pelletized separately in IR grade KBr (Thermo Nicolet Nexus 670 spectrometer), and the spectra were scanned over a range of 4000–500 per cm and recorded in the diffuse reflectance mode at a resolution of 4 per cm. All the spectra were collected in the range 500–4000 per cm.

2.8 | Transmission electron microscopy studies

The size, shape and morphology of AuNPs and AuNPs-Qu-5 were examined using transmission electron microscopy (TEM) (Tecnai G2 F30 S-Twin Microscope, operated at 100 kV).

2.9 | Inductively coupled plasma optical emission spectrometry

Inductively coupled plasma optical emission spectrometry (ICP-OES) is designed to determine the composition of a wide variety of materials. An inductively coupled plasma optical emission spectrometer (ICP-OES, IRIS intrepid II XDL; Thermo Jarrel Ash, Franklin, MA, USA) was used to determine the concentration of metallic gold (Au) in the AuNPs-Qu-5. To perform this experiment, 50 μL of pellet of AuNPs-Qu-5 nanoparticles was mixed with 49.95 mL of mili-Q water and submitted for analysis.

2.10 | Cell line and culture

Oestrogen positive (MCF-7) and oestrogen negative (MDA-MB-231) breast cancer cell lines were obtained from the NCCS (Pune, India). The HUVECs were purchased from Himedia (Mumbai, India). The cells were grown in T25 culture flasks containing DMEM supplemented with 10% FBS and 1% antibiotics (100 U/mL penicillin and 100 μg/mL streptomycin). Cells were maintained at 37°C in a humidified atmosphere containing 5% CO_2. Upon reaching confluency, the cells were trypsinized and passaged.

2.11 | Migration assay (scratch assay)

MCF-7 and MDA-MB-231 cells were plated separately onto six-well culture plates in DMEM containing 10% FBS (2×10^6 cells/well). After 24 hours, the cell monolayer was scraped with a sterile 200 μL micropipette tip to create a wound, washed with PBS and photographed using Nikon inverted microscope, and the images were captured at 10× magnification. Thereafter, the cells were treated with vehicle control DMSO (0.01%), free AuNPs, free quercetin and AuNPs-Qu-5 (50 μM for MCF-7 and 100 μM for MDA-MB-231 cells). After 24 hours treatment period, the plates were photographed using the camera system.

2.12 | Invasion assay

Invasion assay was performed using BD Bio-Coat Matrigel Invasion chamber (USA). Matrigel inserts were rehydrated with serum-free DMEM for 2 hours and 0.5 mL of 5×10^4 MCF-7 and MDA-MB-231 cells were added on the upper chamber. Simultaneously, the vehicle control DMSO (0.01%), free AuNPs, free quercetin and AuNPs-Qu-5 (50 μM for MCF-7 and 100 μM for MDA-MB-231 cells) were also added to the same; 500 μL of DMEM with 10% FBS (as chemoattractant) was added to the lower wells of the invasion chamber in a 24-well plate. After 24 hours, the medium was discarded. Non-migratory cells were removed with cotton-tipped swabs, and the lower surface of the insert was stained with Diff-Quick stain. Further, the cells were counted and captured under a Nikon Eclipse 80i microscope at 10× magnification.

2.13 | Western blot analysis

MCF-7 and MDA-MB-231 cells were treated with free AuNPs, free Qu and AuNPs-Qu-5 (50 μM for MCF-7 and 100 μM for MDA-MB-231). After 24 hours treatment, the cells were lysed in RIPA buffer containing 1X protease inhibitor cocktail. The protein concentrations were determined by Lowry's method (1951).[25] Cell lysate (50 μg) were electrophoresed in 12% SDS polyacrylamide gel and then transferred into PVDF membranes. The membranes were incubated with primary antibodies against p-EGFR, β actin, (1:2000) and VEGFR-2, p-PI3K, Akt, p-Akt, p-GSK-3β, (1:1000) in Tris-buffered saline at 4°C overnight. After washing, the membranes were incubated with HRP-conjugated anti-mouse IgG (1:5000) and goat-anti-rabbit IgG (1:5000). Protein bands

were detected using chemiluminescence system (ECL Kit) and quantified in ChemiDoc XRS Imaging System, Bio-Rad (Irvine, CA, USA).

2.14 | Immunocytochemistry

MCF-7 and MDA-MB-231 cells were cultured in chambered slides (Thermo Scientific Nunc Lab-Tek Chamber Slides, Waltham, MA, USA) and treated with DMEM containing vehicle DMSO (0.01%), free AuNPs, free quercetin and AuNPs-Qu-5 (50 μM for MCF-7 and 100 μM for MDA-MB-231 cells) for 24 hours. Cells were fixed in 4% paraformaldehyde (in PBS) for 15 minutes, washed with PBS (3 × 5 minutes each), incubated for 5 minutes in 0.5% Triton X-100 in PBS and again washed with PBS thrice. The cells were blocked with 5% BSA for 1 hour at room temperature, washed and incubated with primary antibodies for E-cadherin (1:200 dilution), N-cadherin (1:200 dilution) MMP-9 (1:200 dilution) for 3 hour at room temperature. After PBS, washed cells were incubated with secondary antibody conjugated with FITC (EX-465-495), TRITC (EX 540/25) for 1 hour, washed with PBS, stained with nuclear stain DAPI (EX 340-380) for 10 minutes and mounted. The cells were examined using Nikon 80i Eclipse microscope and the images were captured at 40× magnification. Negative controls were used for each experiment to minimize background effect.

2.15 | Co-localization of E-cadherin and vimentin by immunocytochemistry

MDA-MB-231 cells were cultured in chambered slides and treated with DMEM containing vehicle DMSO (0.01%), free AuNPs, free quercetin and AuNPs-Qu-5 (100 μM for MDA-MB-231 cells for all groups) for 24 hours. Cells were fixed in 4% paraformaldehyde (in PBS) for 15 minutes, washed with PBS (3 × 5 minutes each), incubated for 5 minutes in 0.5% Triton X-100 in PBS and again washed thrice with PBS. The cells were blocked with 5% BSA for 1 hour at room temperature, washed and incubated with primary antibodies for E-cadherin and vimentin (1:200 dilution) mixed well, added to the chamber and incubated for 3 hour at room temperature. After washing thrice with PBS, the cells were incubated with secondary antibody conjugated with FITC (EX-465-495), and TRITC (EX 540/25) mixed well then incubated for 1 hour. Then, the cells were washed with PBS, stained with nuclear stain DAPI (EX 340-380) for 10 minutes and mounted. The cells were examined and captured at 40× magnification.

2.16 | In vitro and in vivo angiogenesis study

2.16.1 | Cell viability using MTT assay

Briefly, HUVECs were seeded in 96-well tissue culture plates at a density of 1×10^4 cells/per well. The cells were incubated with different concentrations of free AuNPs (0–125 μM), free Qu (0–125 μM) and AuNPs-Qu-5 (0–125 μM) for 24 hours. Then, 100 μL of 0.5 mg/mL MTT solution was added to each well and incubated at 37°C for 1 hour. Formazan crystals formed were dissolved in dimethyl sulfoxide (100 μL) and incubated in dark for 1 hour. The intensity of the colour developed was recorded using a micro-ELISA plate reader at 570 nm.[26] The number of viable cells was expressed as a percentage of control cells cultured in serum-free medium. Cell viability in control medium without any treatment was represented as 100%. The cell viability is calculated using the formula: % cell viability = (A570 nm of treated cells/A570 nm of control cells) × 100.

2.16.2 | Migration assay (scratch assay)

Human umbilical vein endothelial cells were plated onto six-well culture plates in HiEndo-XLTM Endothelial Cell Expansion Medium (with reduced serum) and were seeded into in a six-well plate coated with 1 mL/well of Matrigel previously polymerized for 1 hour at 37°C. After 24 hours, the cell monolayer was scraped with a sterile 200 μL micropipette tip to create a wound, washed with PBS and examined under inverted microscope. Thereafter, the cells were treated with vehicle DMSO (0.01%), free AuNPs (195 μM), free quercetin (50 μM) and AuNPs-Qu-5 (50 μM of Qu and 195 μM of Au). After 24 hours treatment period, the plates were viewed the same camera system and the images were captured at 10× magnification.

2.16.3 | Invasion assay

Invasion assay was performed using BD Bio-Coat Matrigel Invasion chamber (USA). Matrigel inserts were rehydrated with serum-free HiEndo-XLTM Endothelial Cell Expansion Medium (with reduced serum), for 2 hours followed by addition of 0.5 mL of 5×10^4 HUVECs with serum-free medium in the upper chamber with control (0.01% DMSO), control, free AuNPs (195 μM), free quercetin (50 μM) and AuNPs-Qu-5 (50 μM of Qu and 195 μM of Au for all the groups); 500 μL of HiEndo-XLTM Endothelial Cell Expansion Medium with serum (as chemoattractant) was added to the lower wells of the invasion chamber in a 24-well plate. After 24 hours, the medium was discarded. Non-migratory cells were removed with cotton-tipped swabs, and the lower surface of the insert was stained with Diff-Quick stain. Further, the cells were counted and the images were captured at 20× magnification under the microscope.

2.16.4 | Tube formation assay

Briefly, HUVECs 2×10^4 cells/well into HiEndo-XLTM Endothelial Cell Expansion Medium (with reduced serum) were seeded in a 24-well plate coated with 100 μL/well of Matrigel previously polymerized for 1 hour at 37°C. Cells were incubated for 24 hours in a Thermo-scientific incubator at 37°C in 5% CO_2 atmosphere. The cells were treated in the following manner: control (0.01% DMSO), free AuNPs (195 μM), free quercetin (50 μM) and AuNPs-Qu-5 (50 μM of Qu and 195 μM of Au) for 24 hours. After 24 hours, the cells were washed with plain medium and tube formation was examined and photographed using inverted microscope at 10× magnification (Nikon, Tokyo, Japan).

2.16.5 | VEGFR-2 protein expression by immunocytochemistry

Human umbilical vein endothelial cells were cultured in chambered slides (Thermo Scientific Nunc Lab-Tek Chamber Slides) and treated with HiEndo-XLTM Endothelial Cell Expansion Medium (with reduced serum) containing vehicle DMSO (0.01%), free AuNPs (195 μM), free quercetin (50 μM) and AuNPs-Qu-5 (50 μM of Qu and 195 μM of Au for HUVECs) for a period of 24 hours. Cells were fixed in 4% paraformaldehyde (in PBS) for 15 minutes, followed by washing with PBS (3 × 5 minutes each), incubated for 5 minutes in 0.5% Triton X-100 in PBS and again washed thrice with PBS. The cells were blocked with 5% BSA for 1 hour at room temperature, washed and incubated with primary antibodies for VEGFR-2 (1:200 dilutions) for 3 hours at room temperature. After three washes with PBS, the cells were incubated with secondary antibody conjugated with Alexa Fluor (FITC-EX-465-495) for 1 hour, washed with PBS, counterstained with nuclear stain DAPI (EX 340-380) for 10 minutes and mounted. The cells were examined under microscope. Negative controls were used for each experiment to minimize background effect, and the images were captured at 40× magnification.

2.16.6 | Chick embryo angiogenesis assay

The fertile eggs of brown leghorn were procured from government poultry (Directorate of Poultry Research, Hyderabad and Rajendra Nagar) and incubated in an egg incubator. On the fourth day of incubation, the shell was peeled on the top and a small window was created. Sterile filter papers discs were soaked in the drug, Control (miliQ-water) free AuNPs (195 μM), free quercetin (50 μM) and AuNPs-Qu-5 (50 μM of Qu and 195 μM of Au for all the groups) were placed around the blood vessels in the window area. The treated eggs were incubated in horizontal egg incubators (Southern) at 37°C and 60–70% RH. The images were captured at 0 and 4 hours post treatments with a camera attached to stereo microscope. The blood vessels inhibition in response to treatment was quantified using Angioquant software.[27,28]

2.16.7 | In vivo anti-tumour model and treatment

The animals were fed with standard pellet diet (Lipton India Ltd, Mumbai, India). Experiment was approved by the Institute Animal Ethical Committee (IAEC-No 01/13/14). Breast cancer model was established in female Sprague-Dawley rats using 25 mg of 7, 12-dimethyl benz(a)anthracene (DMBA) dissolved in 0.5 mL of corn oil, administered through gastric intubation.[29] After DMBA administration, the rats were examined regularly to observe the appearance of tumour. After 60 days, the tumour appearance was confirmed by histopathological examination. Once the tumour appears, the animals were divided into four groups: Group 1, DMBA-induced control animals; Group 2, DMBA-induced animals treated with free AuNPs (25 mg/kg, bw); Group 3, DMBA-induced breast cancer animals treated with free Qu (25 mg/kg, bw); Group 4, DMBA-induced breast cancer animals treated with AuNPs-Qu-5 (25 mg/kg, bw) by intratumoural injection for 8 days. At the end of the experimental period, all animals were

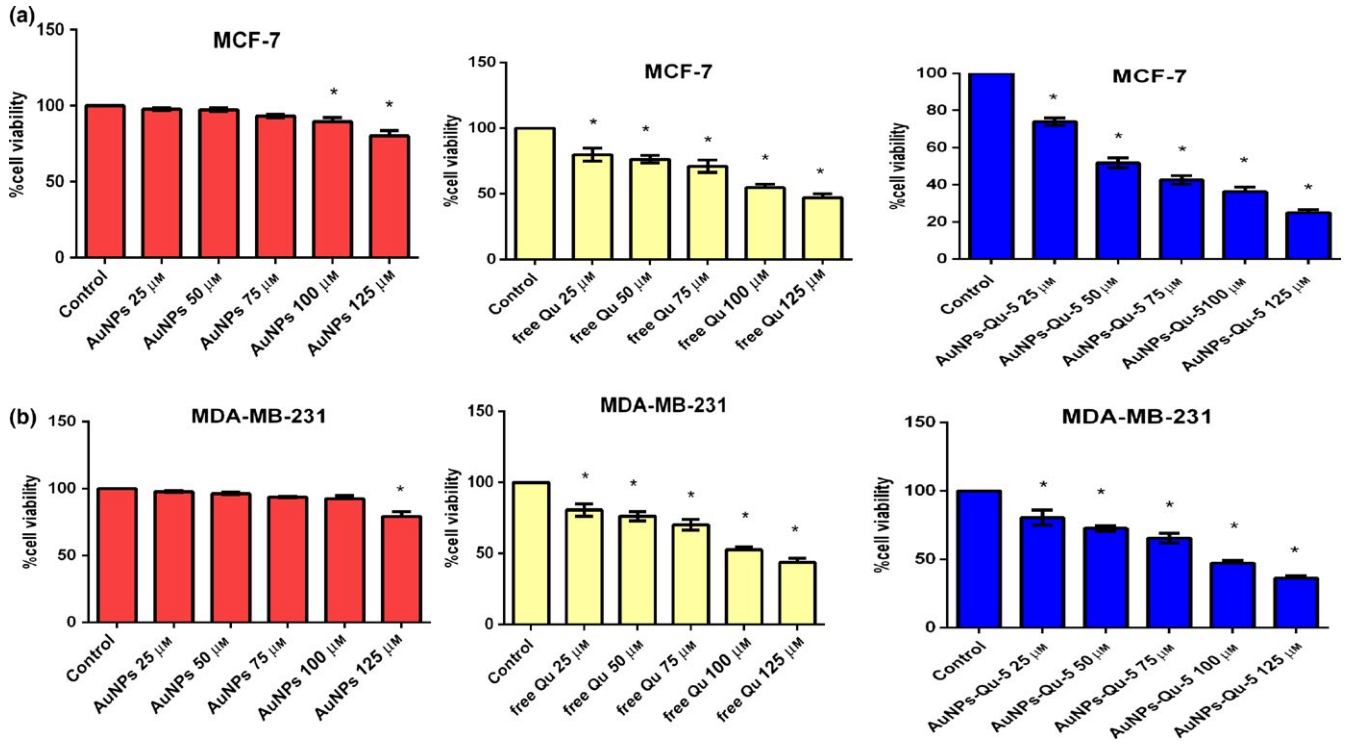

FIGURE 1 In vitro anticancer efficacy of free AuNPs, free quercetin and AuNPs-Qu-5 assessed by MTT assay using MCF-7 and MDA-MB-231 cell lines treated for 24 h. Each bar represents the mean ± SEM of six independent observations. '*' represents statistical significance between control vs treatment groups

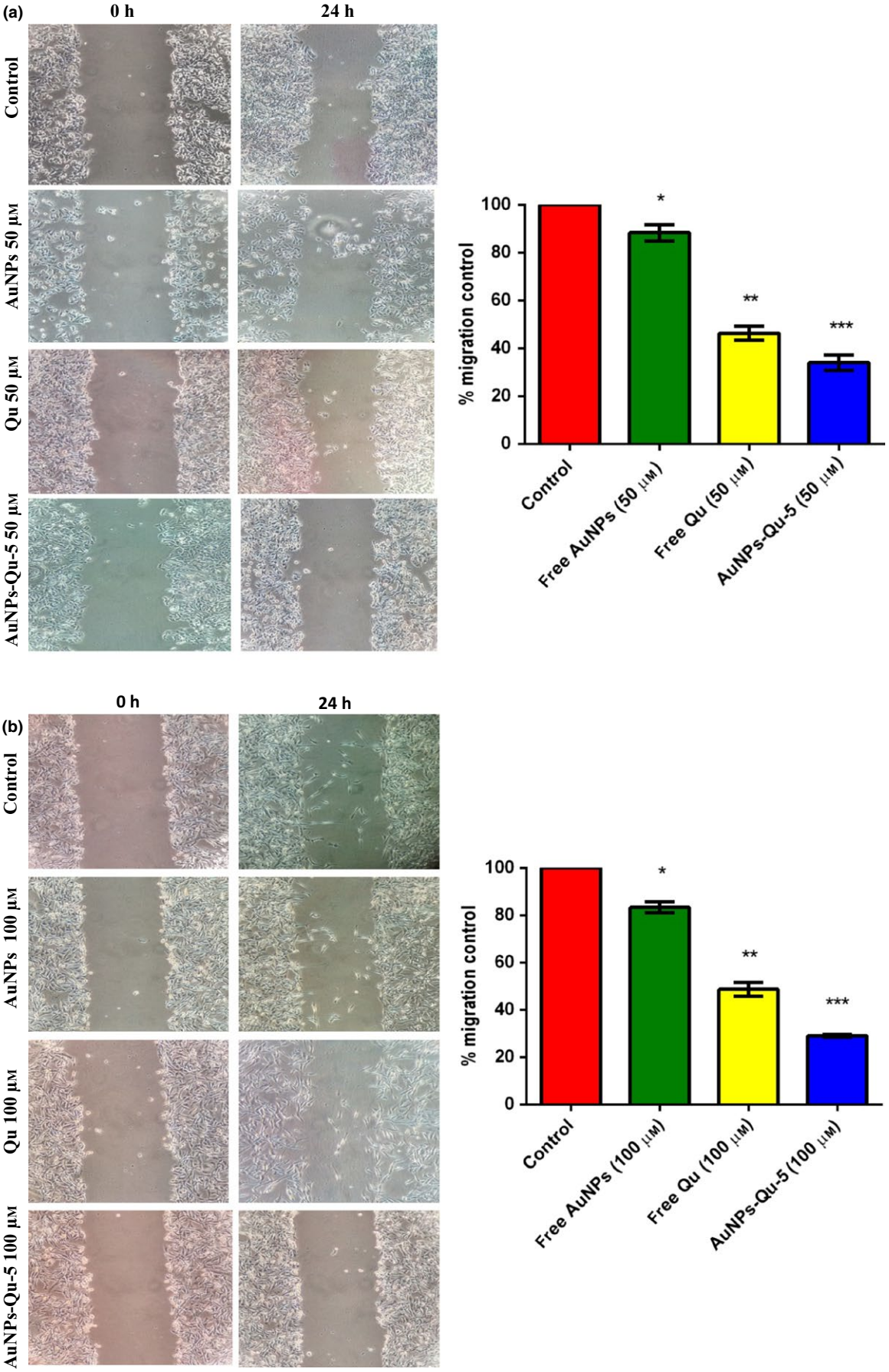
(a)
0 h
24 h
Control
AuNPs 50 µM
Qu 50 µM
AuNPs-Qu-5 50 µM
% migration control
100
80
60
40
20
0
*
**
***
Control
Free AuNPs (50 µM)
Free Qu (50 µM)
AuNPs-Qu-5 (50 µM)
(b)
0 h
24 h
Control
AuNPs 100 µM
Qu 100 µM
AuNPs-Qu-5 100 µM
% migration control
100
80
60
40
20
0
*
**
***
Control
Free AuNPs (100 µM)
Free Qu (100 µM)
AuNPs-Qu-5 (100 µM)

FIGURE 2 (a) Effect of AuNPs-Qu-5 on cell migration in MCF-7 cells. The number of cells migrated was counted manually and percentage of cells migrated was plotted, and the respective histogram is shown. Each bar represents the mean ± SEM of three independent observations: "*" control vs others; "**" free AuNPs vs others and "***" Qu vs AuNPs-Qu-5 (10× magnification). (b) Effect of AuNPs-Qu-5 on cell migration in MDA-MB-231 cells. The number of cells migrated was counted manually and percentage of cells migrated was plotted, and the respective histogram is shown. Each bar represents the mean ± SEM of three independent observations: "*" control vs others; "**" free AuNPs vs others and "***" Qu vs AuNPs-Qu-5 (10× magnification)

killed by cervical decapitation. The breast tumours were excised immediately and rinsed with ice-cold physiological saline, and tumours were further fixed in formalin for histopathology examination.

2.17 | Statistical analysis

Data were expressed as mean ± SEM. Statistical analyses were performed using one-way analysis of variance (ANOVA) followed by Student–Newman–Keul's (SNK) test for comparison between treatment values and control values using Prism software. $P<.05$ was considered to be statistically significant.

3 | RESULTS

3.1 | UV-visible spectroscopy

UV-visible spectroscopy was used to check the formation of AuNPs and AuNPs-Qu-5 and the attachment of Qu with AuNPs. The AuNPs

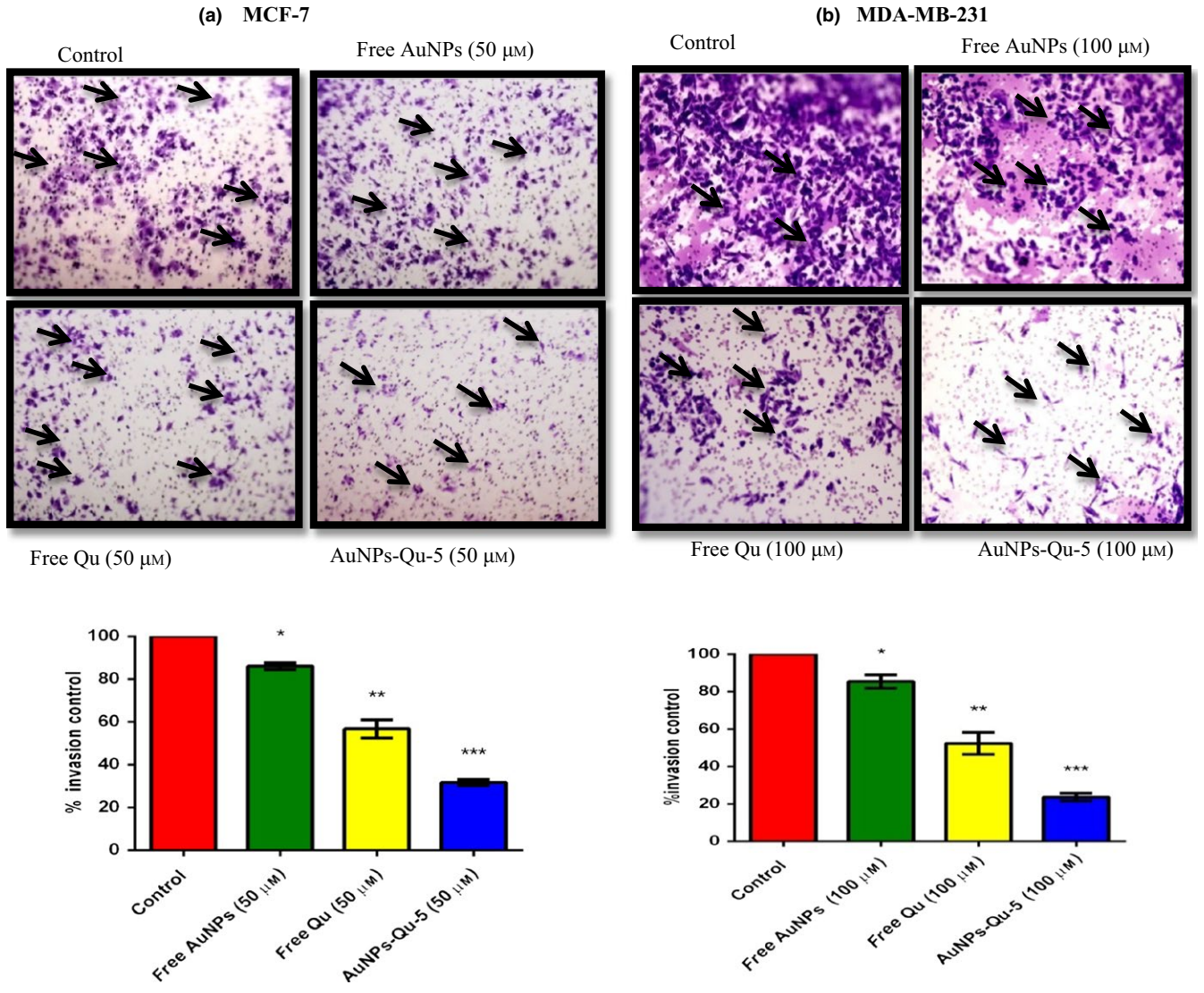

FIGURE 3 Effect of AuNPs-Qu-5 on cell invasion: (a) MCF-7 and (b) MDA-MB-231 cells. The number of cells invaded was counted manually and percentage of cells invasion was plotted, and the respective histogram is shown. Black arrows indicate the number of cells invaded. Each bar represents the mean ± SEM of three independent observations: "*" control vs others; "**" free AuNPs vs others and "***" Qu vs AuNPs-Qu-5 (20× magnification)

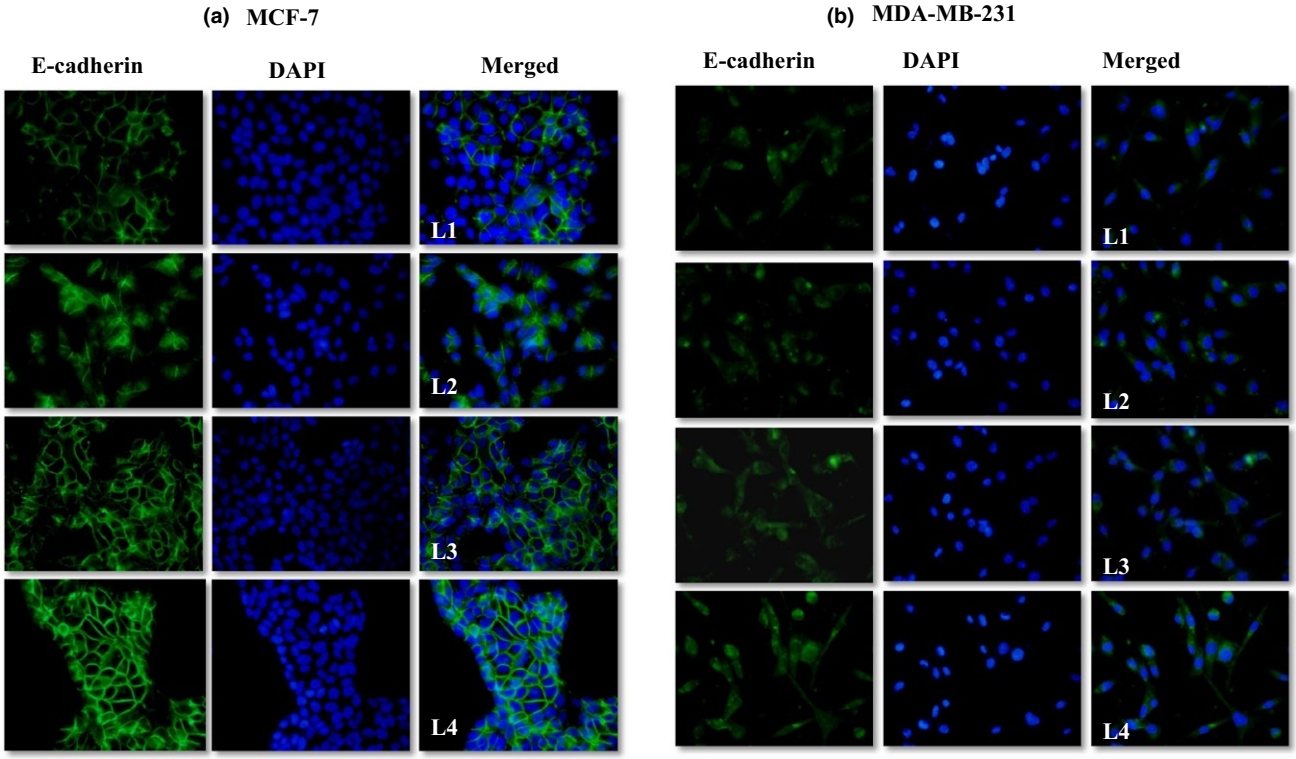

L1- vehicle control, L2- AuNPs (50 μM), L3- free quercetin (50 μM) and L4- AuNPs-Qu-5 (50 μM) treated.

L1- vehicle control,L2- AuNPs (100 μM), L3- free quercetin (100 μM) and L4- AuNPs-Qu-5 (100 μM) treated.

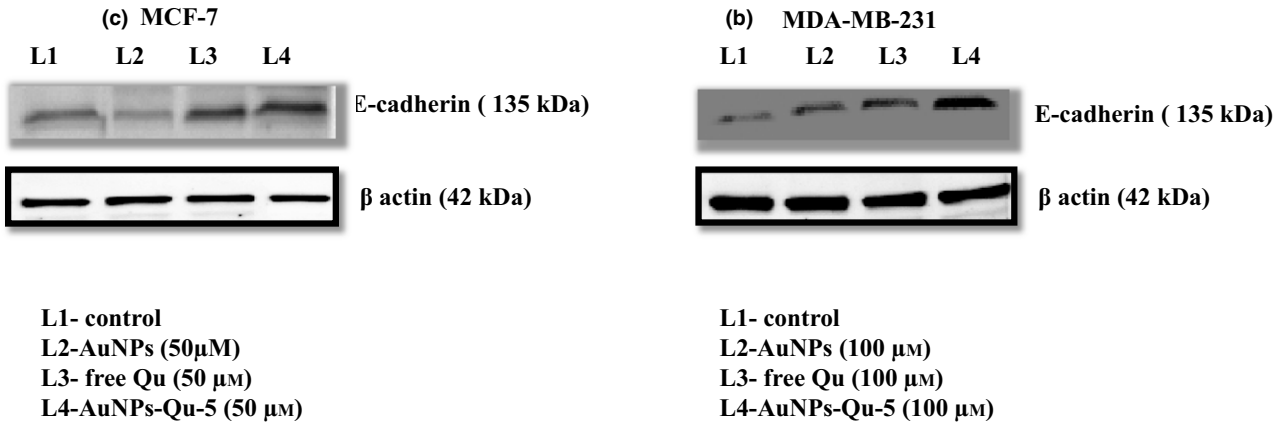

L1- control
L2-AuNPs (50μM)
L3- free Qu (50 μM)
L4-AuNPs-Qu-5 (50 μM)

L1- control
L2-AuNPs (100 μM)
L3- free Qu (100 μM)
L4-AuNPs-Qu-5 (100 μM)

FIGURE 4 (a, b) Effect of free Qu and AuNPs-Qu-5 on protein expression of E-cadherin in MCF-7 and MDA-MB-231 cells. Protein expression of E-cadherin (Green fluorescence) counterstained by DAPI (blue colour nuclear stain) by immunocytochemistry. The images were captured at 40× magnification. (c, d) Effect of free Qu and AuNPs-Qu-5 on AuNPs-Qu-5 on protein expression of E-Cadherin in MCF-7 and MDA-MB-231 cells using Western blot

showed the absorption spectra at λ_{max} ~ 507 nm, generally attributed to the surface plasmon excitation of small spherical sized AuNPs (Supplementary Fig. 1a). The wavelength at maximum absorbance of AuNPs-Qu-5 showed considerable shift (λ_{max} ~ 520 nm) from the naked AuNPs (λ_{max} ~ 507 nm), indicating attachment of the drug molecule on AuNPs surfaces (Supplementary Fig. 1a). This result indicates the change in the properties of AuNPs by the physical association of Qu, on AuNPs surfaces. The Qu shows the absorbance maximum at λ_{max} ~ 379.5 nm. Additionally, the % binding of Qu was calculated from the standard curve of Qu using UV-visible spectroscopy. Around 75% of Qu was attached with AuNPs in AuNPs-Qu-5 pellets calculated from standard curve of Qu (Supplementary Fig. 1b).

3.2 | DLS (Dynamic light scattering) study

The DLS technique was used to determine the size of nanoparticles. The hydrodynamic radii of AuNPs and AuNPs-Qu-5 were measured as 10.22 nm (Supplementary Fig. 2a) and 18.13 nm (Supplementary Fig. 2b), respectively, using DLS. The comparatively large size of AuNPs-Qu-5 as observed in DLS indicated the attachment of the Qu on AuNPs surface. PDI of AuNPs and

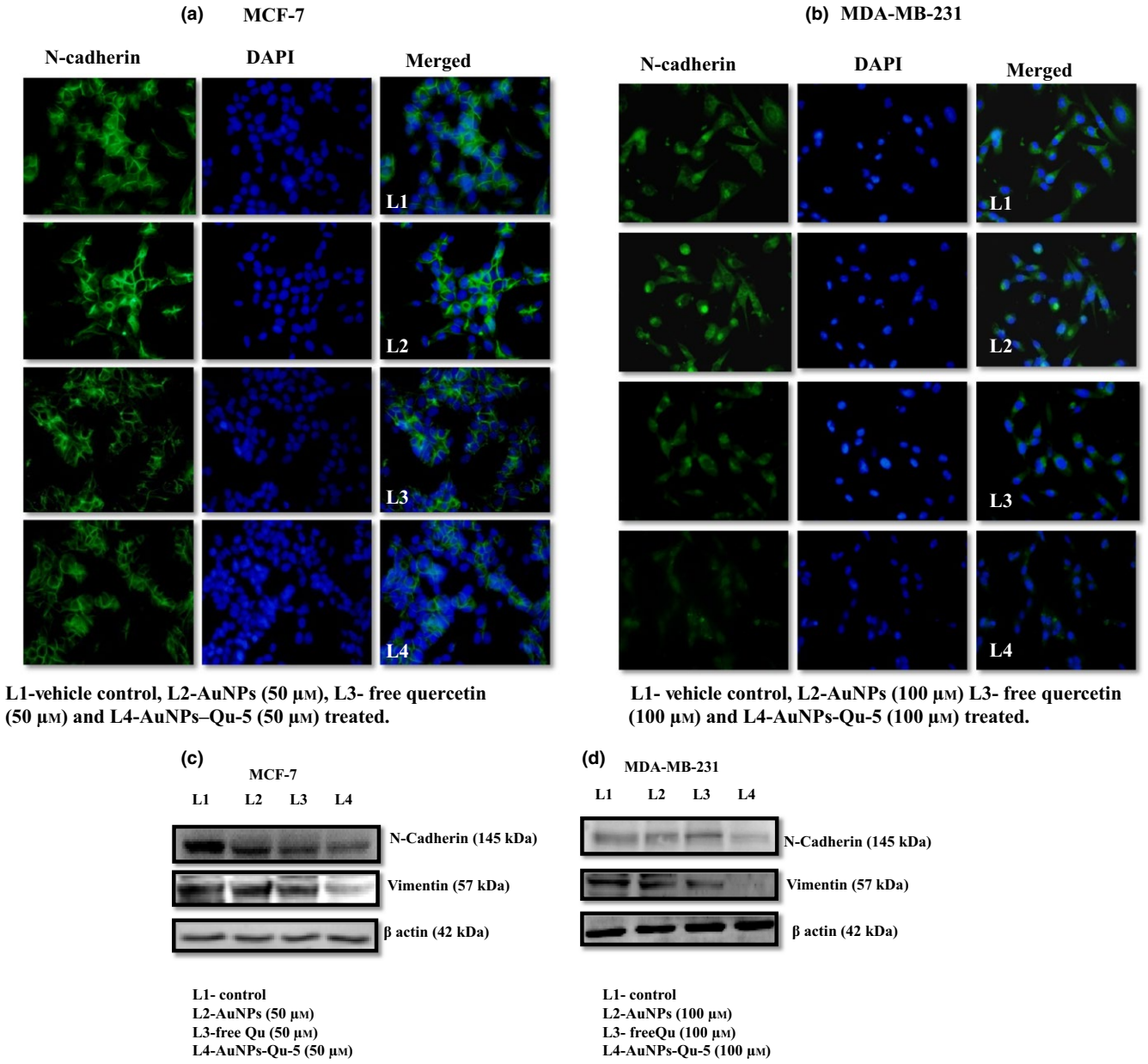

FIGURE 5 (a, b) Effect of free Qu and AuNPs–Qu-5 on the protein expression of N-cadherin in MCF-7 and MDA-MB-231 cells. Protein expression of N-cadherin (green fluorescence) counterstained by DAPI (blue colour nuclear stain) by immunocytochemistry. The images were captured at 40× magnification. (c, d) Effect of free Qu and AuNPs-Qu-5 on protein expression of N-Cadherin and vimentin in MCF-7 and MDA-MB-231 cells using Western blot

AuNPs-Qu-5 were 0.22 and 0.26, respectively. This indicates well dispersibility of both AuNPs and AuNPs-Qu-5 nanoparticles/nanoconjugates.

3.3 | Fourier transformed infrared (FTIR) spectroscopy

The characteristic stretching vibration of C=O (Supplementary Fig. 3a) was observed at 1666 per cm for Qu that shifted to 1646 per cm in case of AuNPs-Qu-5 (Supplementary Fig. 3b) with reduced intensity, indicating the formation of stable conjugation of C=O with AuNPs.[30,31] A strong stretching vibration peak of phenolic –OH group was found at 3398 per cm in Qu, which was shifted to higher wave numbers (3425 per cm) in AuNPs-Qu-5, indicating the possible dative bonding between Au and –OH (Supplementary Fig. 3b).[32] FT-IR studies thus proved that Qu was conjugated with AuNPs through the interaction between Au with polar –OH group of Qu.

3.4 | Transmission electron microscope studies

In order to find the size, shape and morphology of AuNPs and AuNPs-Qu-5, TEM analysis was carried out. The TEM images of the free AuNPs showed spherical-shaped gold nanoparticles with average size of 3.5 nm. AuNPs-Qu-5 showed nearly monodispersed spherical

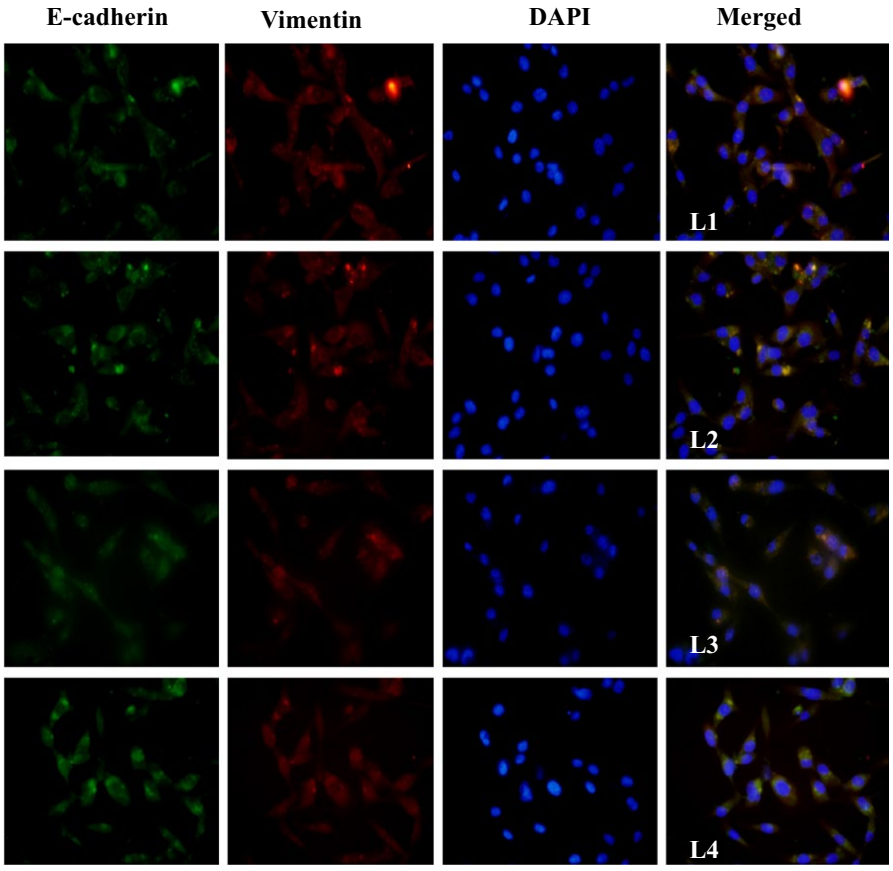

FIGURE 6 Effect of free Qu and AuNPs-Qu-5 on E-cadherin and vimentin co-localized protein expression in MDA-MB-231 cells. Protein expression of E-cadherin (green) and vimentin (red) (red and green fluorescence) counterstained by DAPI (blue colour nuclear stain) by immunocytochemistry. The images were captured at 40× magnification

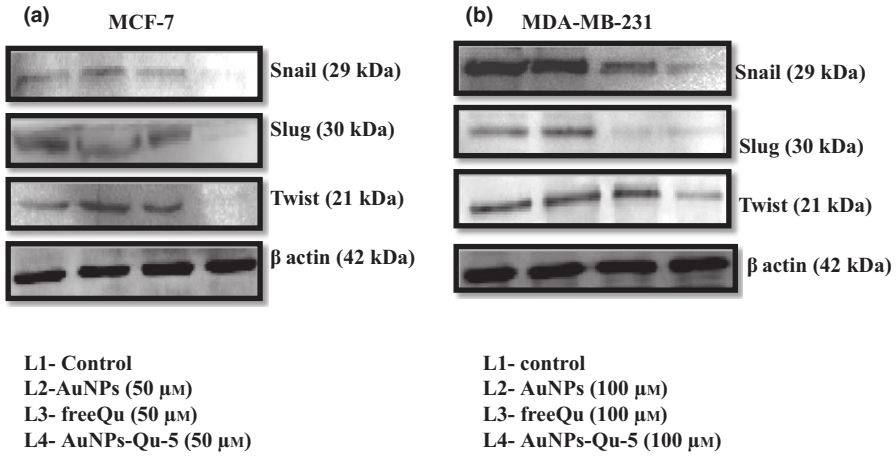

FIGURE 7 (a, b) Effect of free Qu and AuNPs-Qu-5 on protein expression of Snail, Slug and Twist in MCF-7 and MDA-MB-231 cells using Western blot

nanoparticles with average size of 5.2 nm, calculated from size distribution plot (Supplementary Fig. 3c).

3.5 | In vitro anticancer studies

Cell viability of free AuNPs, free Qu and AuNPs-Qu-5 was checked on breast cancer cell lines (MCF-7 and MDA-MB-231), and it was found that free AuNPs did not show any cytotoxicity towards cancer cell lines. However, free Qu and AuNPs-Qu-5 decreased the cell viability. AuNPs-Qu-5 showed IC_{50} value at 50 μM in MCF-7 cells and AuNPs-Qu-5 treated MDA-MB-231 cells showed IC_{50} at 100 μM for 24 hours (Fig. 1a,b). The concentration mentioned here represents the concentration of Qu in free drug and AuNPs-Qu-5 nanoconjugates. Furthermore, the gold concentration was calculated with the help of ICP-OES analysis in the 50 μM AuNPs-Qu-5 was recorded as 195 μM.

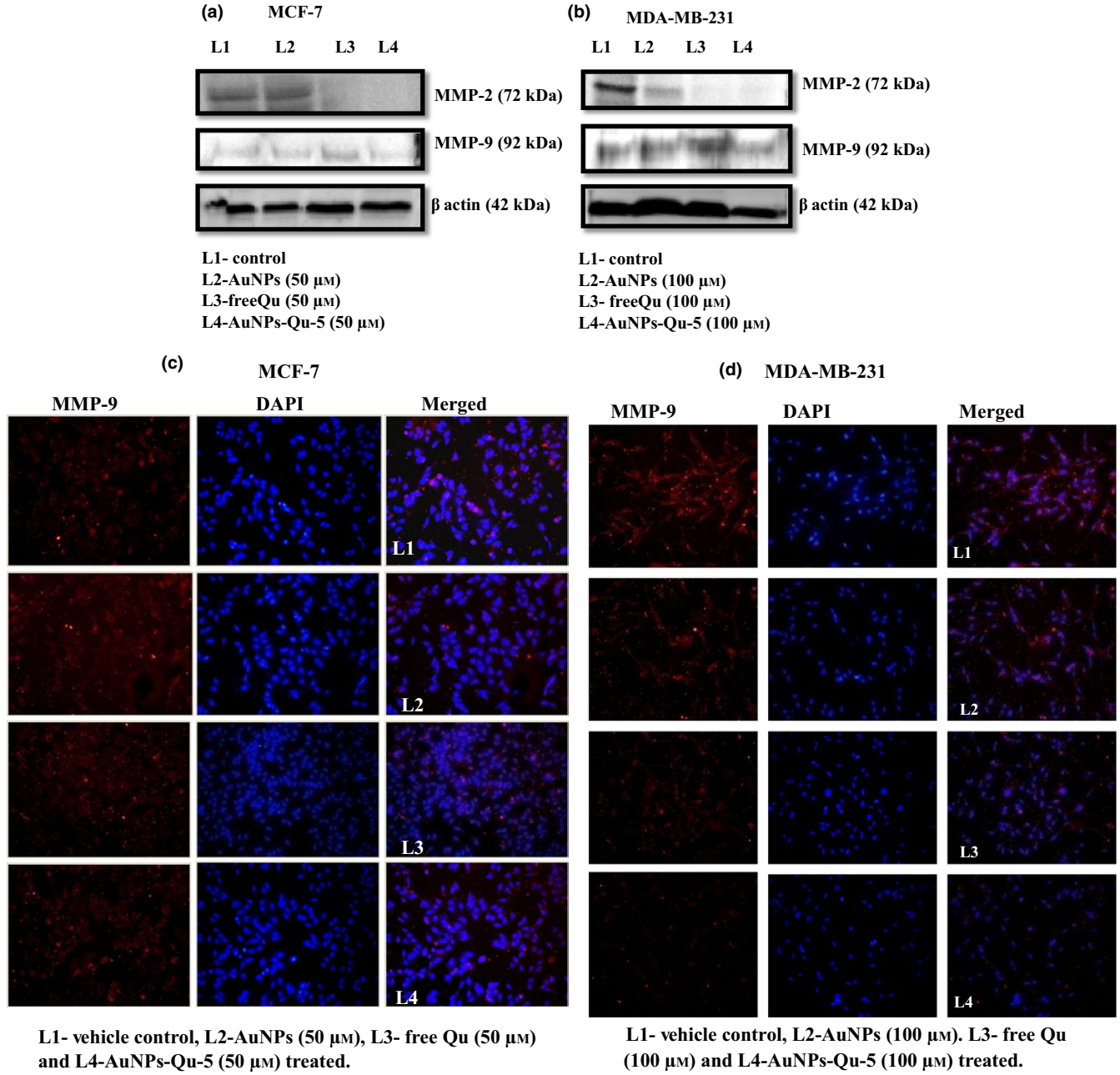

FIGURE 8 (a, b) Effect of free Qu and AuNPs–Qu-5 on the protein expression of MMP-2 and MMP-9 in MCF-7 and MDA-MB-231 cells using Western blot. (c, d) Effect of free Qu and AuNPs-Qu-5 on the protein expression of MMP-9 in MCF-7 and MDA-MB-231 cells. Protein expression of MMP-9 (Red fluorescence), counterstained by DAPI (blue colour nuclear stain) by immunocytochemistry. The images were captured at 40× magnification

3.6 | Effect of AuNPs-Qu-5 on cell migration and invasion assay

To determine the effect of AuNPs-Qu-5 on EMT in breast cancer cells, this study investigated migration and invasion of MCF-7 and MDA-MB-231 cells in the presence and absence of AuNPs, free Qu and AuNPs-Qu-5 by wound-healing/scratch assay and invasion assay. The images were taken before (0 hour) and after (24 hours) the treatment. In control and AuNP-treated group, more number of cells were invaded and migrated. But AuNPs-Qu-5 treatment significantly decreased the migration and invasiveness of MCF-7 and MDA-MB-231 cells compared with free Qu (Figs 2a,b & 3a,b), suggesting that AuNPs-Qu-5 is more effective than free Qu in curtailing the migration and invasion of breast cancer cells.

3.7 | Effect of AuNPs-Qu-5 on EMT regulatory genes

To determine the effect of free Qu and AuNPs-Qu-5 on the EMT at the molecular level, we screened EMT marker expression by Western blotting and immunocytochemistry. E-cadherin protein expression

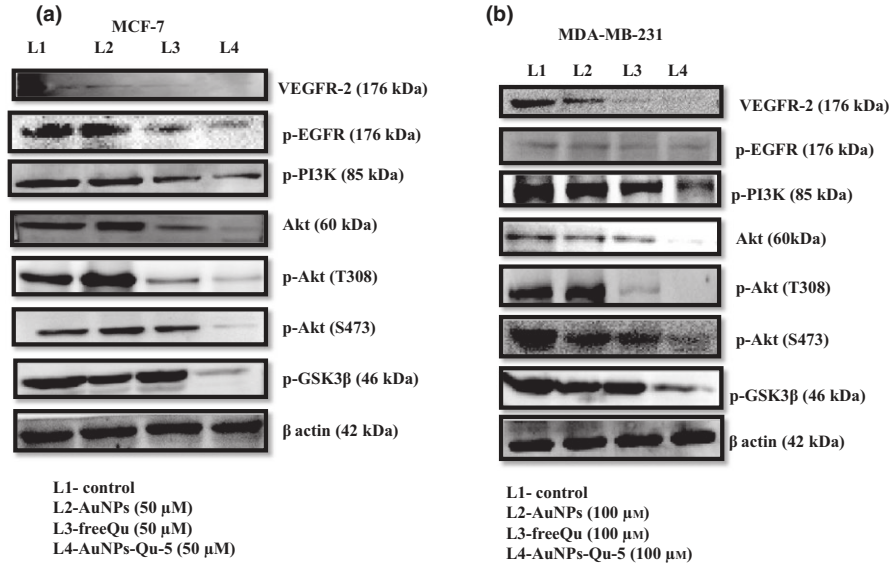

FIGURE 9 (a, b) Effect of free Qu and AuNPs-Qu-5 on protein expression of VEGFR-2/p-EGFR/p-PI3K/Akt/p-GSK3β in MCF-7 and MDA-MB-231 cells using Western blot

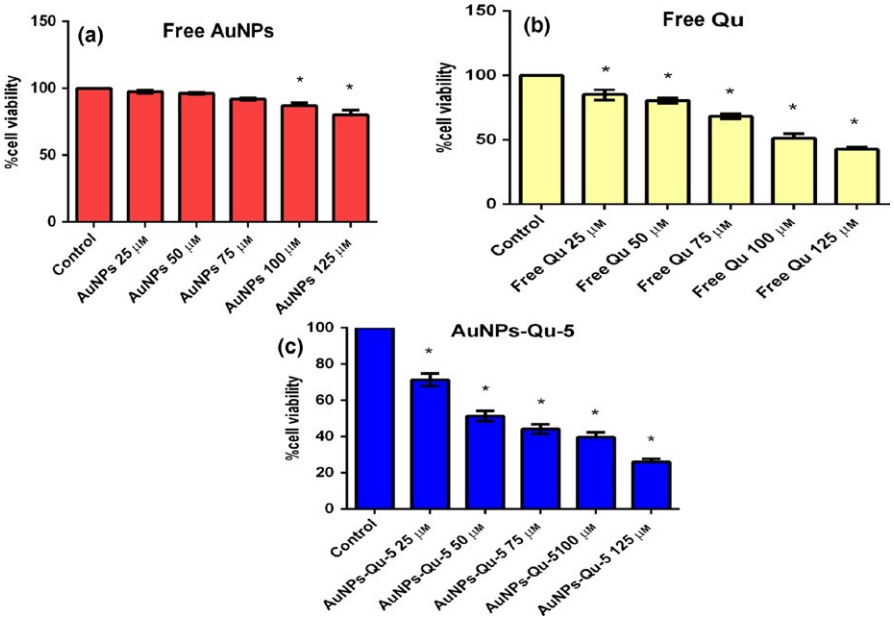

FIGURE 10 (a–c) Effect of free AuNPs, free Qu and AuNPs-Qu-5 on the cell viability of HUVECs by MTT assay. Each value represents the mean ± SEM of six independent observations. $P<.05$ was considered to be statistically significant. "*" represents statistical significance between control vs other treatment groups

was up-regulated in treatment with AuNPs-Qu-5 (Fig. 4a–d & Fig. 6), whereas N-cadherin and vimentin protein expression was down-regulated in MCF-7 and MDA-MB-231 cells compared with free Qu (Fig. 5a–d & Fig. 6). Therefore, the reduced migratory and invasive property of AuNPs-Qu-5 treatment is likely due to modulation of EMT-related protein expression.

3.8 | Effect of AuNPs-Qu-5 on transcriptional repressor factors

The molecular abnormalities behind the elevated E-cadherin expression were assessed by evaluating the protein expression of transcriptional repressors, including Snail, Slug and Twist. We observed that

FIGURE 11 (a) Effect of free Qu and AuNPs-Qu-5 on cell migration in HUVECs. Cells were scratched with a pipette tip and washed twice with PBS and photographed (0 h). Scratched HUVECs were treated with free AuNPs, free Qu and AuNPs-Qu-5 for 24 h. The number of cells migrated were counted manually and percentage of cells migrated was plotted, and the respective histogram is shown. Each bar represents the mean ± SEM of three independent observations: "*" control vs others; "**" free AuNPs vs others and "***" Qu vs AuNPs-Qu-5 (10× magnification). (b) Effect of free Qu and AuNPs-Qu-5 on cell invasion in HUVECs. The number of cells invaded was counted manually and percentage of cells invasion was plotted, the respective histogram is shown. Black arrows indicate the number of cells invaded. Each bar represents the mean ± SEM of three independent observations: "*" control vs others; "**" free AuNPs vs others and "***" Qu vs AuNPs-Qu-5 (20× magnification)

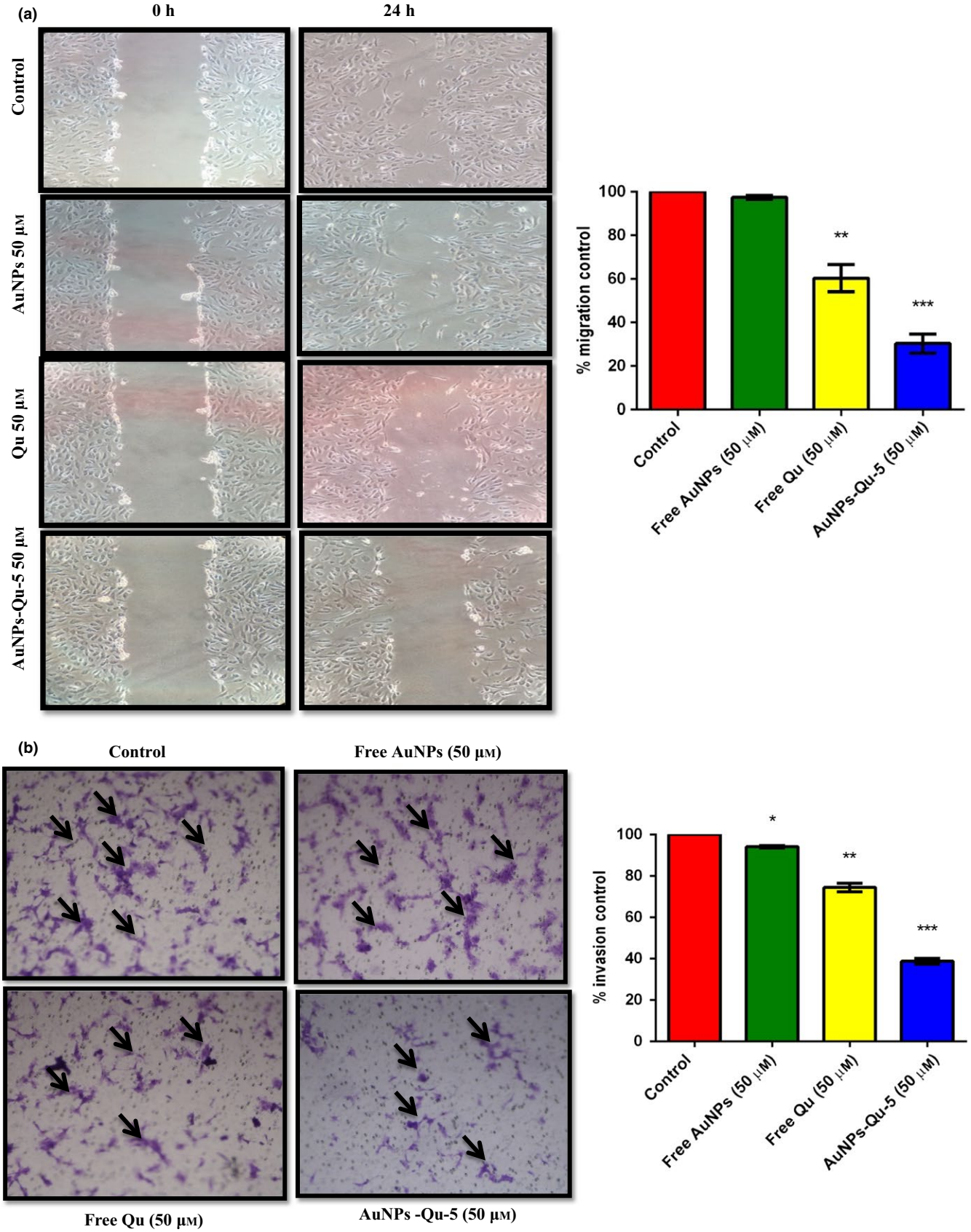
(a)
0 h
24 h
Control
AuNPs 50 µM
Qu 50 µM
AuNPs-Qu-5 50 µM
% migration control
100
80
60
40
20
0
**
***
Control
Free AuNPs (50 µM)
Free Qu (50 µM)
AuNPs-Qu-5 (50 µM)
(b)
Control
Free AuNPs (50 µM)
Free Qu (50 µM)
AuNPs -Qu-5 (50 µM)
% invasion control
100
80
60
40
20
0
*
**
***
Control
Free AuNPs (50 µM)
Free Qu (50 µM)
AuNPs-Qu-5 (50 µM)

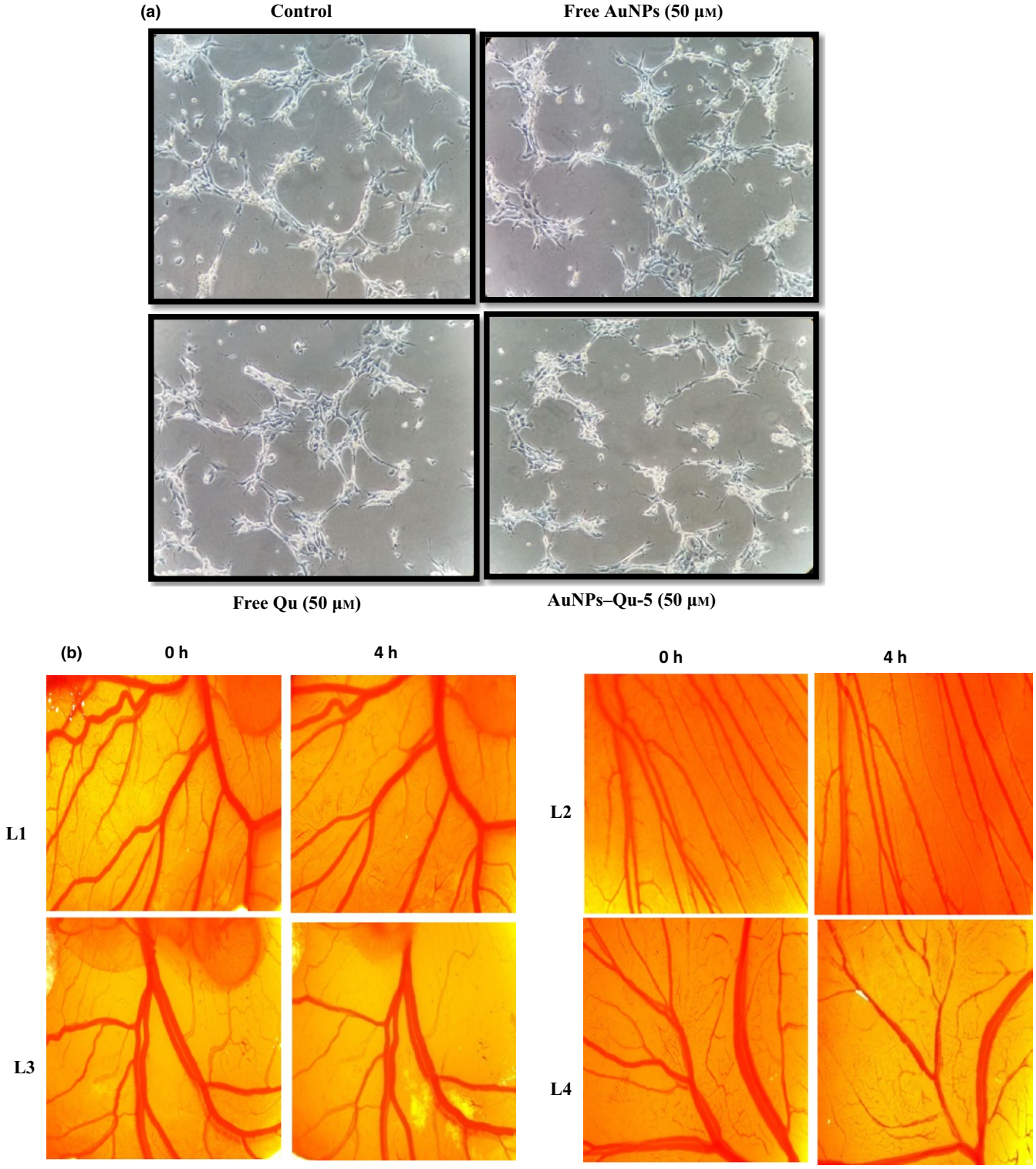

FIGURE 12 (a) Effect of free Qu and AuNPs–Qu-5 on capillary like tube formation in HUVECs. HUVECs were seeded in matrigel coated plates and cells were treated with free AuNPs, free Qu and AuNPs-Qu-5 for 24 h. Tube formation was observed by microscopy and photographed (10× magnification). (b) Effect of free Qu and AuNPs-Qu-5 on Chick embryo angiogenesis (CEA) assay. Ex vivo angiogenesis assay in a chick embryo model incubated with control, free AuNPs, free Qu and AuNPs-Qu-5 respectively. The results demonstrate that AuNPs-Qu-5 inhibits the neovascularization in chick model of angiogenesis. L1, control; L2, AuNPs; L3, free Qu, L4, AuNPs-Qu-5

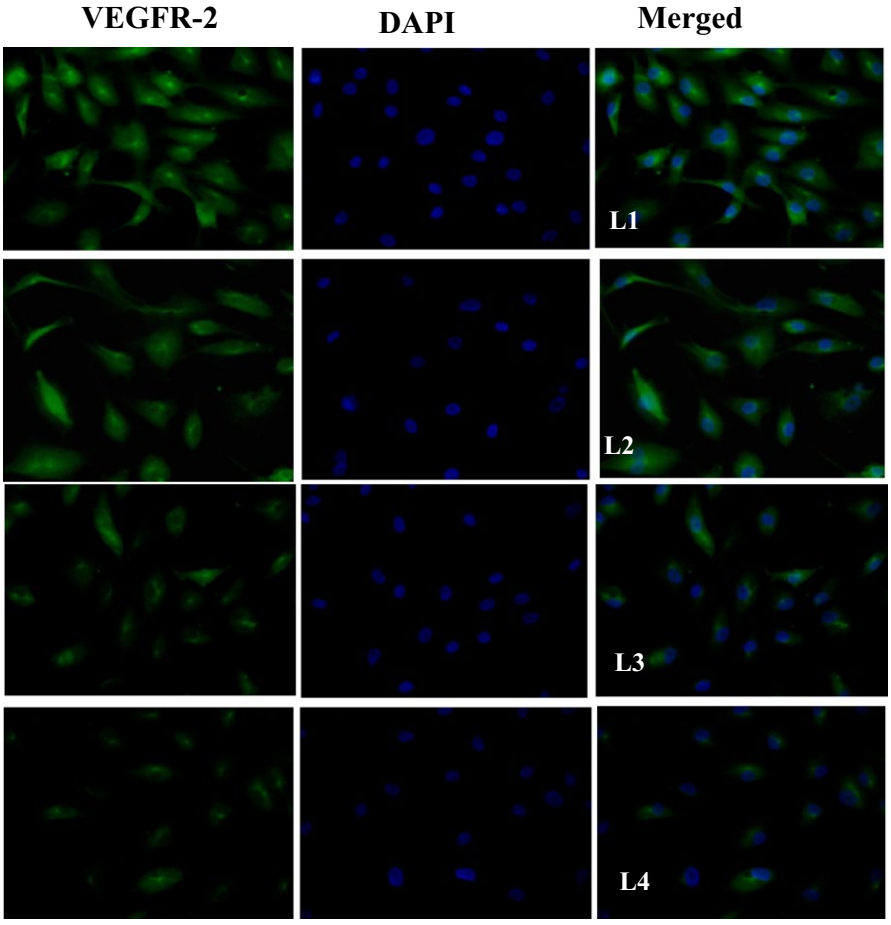

FIGURE 13 Effect of free Qu and AuNPs-Qu-5 on the protein expression of VEGFR-2 in HUVECs. Protein expression of VEGFR-2 (Green fluorescence), counterstained by DAPI (blue colour nuclear stain) by immunocytochemistry. All the images were taken in 40× magnification. L1, vehicle control; L2, AuNPs (50 μM); L3, free Quercetin (50 μM); and L4, AuNPs-Qu-5 (50 μM) treated (40× magnification)

treatment with AuNPs-Qu-5 suppressed the transcriptional repressors protein levels in MCF-7 and MDA-MB-231 cells compared with free Qu (Fig. 7a,b). Thus, our results suggest that AuNPs-Qu-5 inhibits the EMT at molecular level.

3.9 | Effect of AuNPs-Qu-5 on MMP-2 and MMP-9

Matrix metalloproteinases (MMPs) degrade structural components of the ECM, which allows tumour invasion and metastasis. MMP-2 and MMP-9 play an important role in the processes of invasive metastasis and tumour angiogenesis. We investigated the protein expression of MMP-2 and MMP-9 by Western blot and immunocytochemistry. AuNPs-Qu-5 inhibited the action of MMP-2 and MMP-9 in MCF-7 and MDA-MB-231 cells compared with free Qu (Fig. 8a–d).

3.10 | Effect of AuNPs-Qu-5 on p-EGFR/VEGFR--2/p-PI3K/Akt/p-Akt/p-GSK3β pathway

EGFR-mediated PI3K/Akt signalling pathways are involved in EMT process. We investigated the protein expression of p-EGFR/VEGFR-2/p-PI3K/Akt/p-Akt/p-GSK-3β. Our results showed that AuNPs-Qu-5 inhibits p-EGFR/VEGFR-2 protein expression as well as the downstream signalling molecules of p-PI3K/Akt/p-Akt/p-GSK-3β protein expression in MCF-7 and MDA-MB-231 cells compared with free Qu (Fig. 9a,b).

3.11 | Effect of AuNPs-Qu-5 on cytotoxicity, migration and invasion in HUVECs

Endothelial cells are currently used as in vitro model system for various physiological and pathological screening, especially in angiogenesis studies. Hence, we investigated the cytotoxicity effect of AuNPs-Qu-5 on HUVEC cytotoxicity, by performing anti-migration and anti-invasion assays. Blank gold nanoparticle–treated cells did not show cytotoxicity in HUVECs, which shows biocompatibility of AuNPs (Fig. 10a); whereas AuNPs-Qu-5 treatment decreased cell viability of HUVECs in a dose-dependent manner compared with free Qu treatment (Fig. 10b,c). Treatment with AuNPs-Qu-5 showed higher cytotoxicity, which was observed at 50 μM than free Qu 100 μM. Further, we studied the effect of AuNPs-Qu-5 on migration and invasion of HUVECs. We found that AuNPs-Qu-5 exhibited anti-angiogenic activity, and it significantly inhibited the endothelial cell migration and invasion in HUVECs as compared with free Qu (Fig. 11a,b).

3.12 | Effect of AuNPs-Qu-5 on in vitro and in vivo angiogenesis

Angiogenesis is a key player for tumour growth and progression. In addition to the impact of AuNPs-Qu-5 on EMT, we also investigated its effect on anti-angiogenesis using HUVEC model. Our results showed that AuNPs-Qu-5 inhibits the in vitro angiogenesis by suppressing

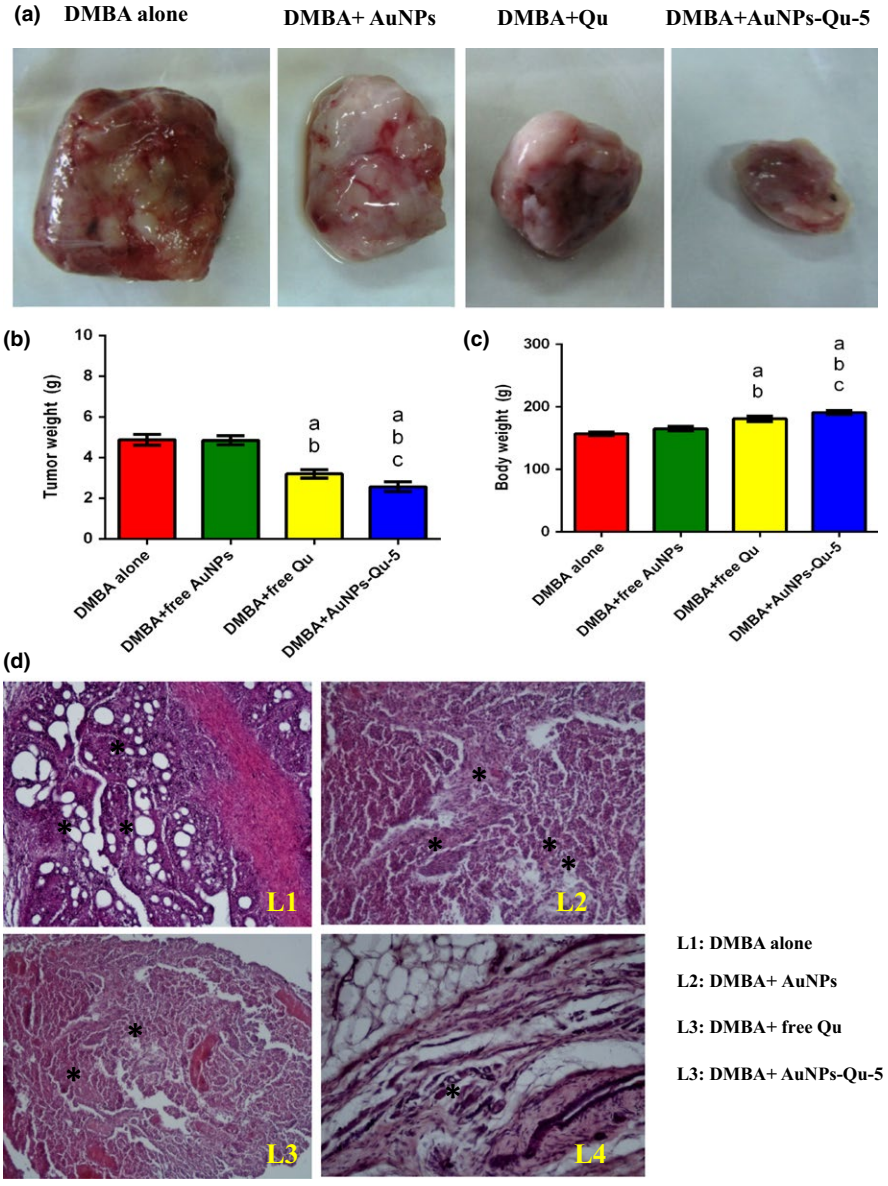

FIGURE 14 Effect of free Qu and AuNPs-Qu-5 on DMBA-induced mammary carcinoma in Sprague-Dawley rats. AuNPs-Qu-5 inhibited the DMBA-induced tumour growth in Sprague-Dawley rats: (a) Representative photographs of breast tumours in each group; (b) weight of breast tumours in each group; (c) body weight of all the animals in each group. "a" DMBA alone vs others; "b" DMBA induced animals +free AuNPs vs others; and "c" DMBA induced animals + free Qu. (d) Effect of free Qu and AuNPs-Qu-5 on histopathological examination. (d) Histopathological examination of DMBA-induced breast cancer in Sprague-Dawley rats. Histopathological changes in the mammary tissues of cancer-induced vehicle and experimental animals (haematoxylin and eosin, 10×). L1: Cancer-induced breast cancer animals show the extensive solid areas and several neoplastic cells lobular structural disruption; L2: CI + free AuNPs show extensive solid tumour; L3: free quercetin-treated animal shows few amount of neoplastic structure; L4: AuNPs-Qu-5-treated animal shows normal mammary epithelial cells appearance. *Represent neoplastic cells in DMBA-induced group

the capillary-like tube formation in HUVECs compared with free Qu (Fig. 12a). Furthermore, we confirmed the anti-angiogenesis effect of AuNPs-Qu-5 ex vivo by employing CEA assay. This study revealed that AuNPs-Qu-5 inhibits neovascularization compared with free Qu (Fig. 12b). Taken together, both in vitro and in vivo results demonstrated that AuNPs-Qu-5 can inhibit angiogenesis more efficiently compared with free Qu.

3.13 | Effect of AuNPs-Qu-5 on VEGFR-2 protein expression in HUVECs

To investigate the mechanism of AuNPs-Qu-5 effect on angiogenesis, we investigated VEGFR-2 protein expression in HUVECs by immunocytochemistry. Our results show that at 50 μM, AuNPs-Qu-5 inhibits the expression of VEGFR-2 protein expression in HUVECs compared with free Qu (Fig. 13).

3.14 | Effect of AuNPs-Qu-5 on DMBA-induced mammary carcinoma

DMBA-induced breast cancer animals showed a significant decrease in body weight, whereas in treatment with free Qu and AuNPs-Qu-5, the body weight was increased. AuNP-alone-treated tumour-bearing rats did not exhibit anti-tumour activity. However, AuNPs-Qu-5-treated rats were more efficient in suppressing tumour growth. Remarkably, the AuNPs-Qu-5 treatment also prolonged the survival of tumour-bearing rats compared with free quercetin-treated rats (Fig. 14a–d). In addition, histological examination of mammary gland in DMBA-induced animals showed several neoplastic cell and disturbed lobular structure. However, AuNPs-Qu-5 treatment restored the architecture of epithelial mammary tissue to near normal compared with treatment with free Qu.

4 | DISCUSSION

Gold nanoparticle–conjugated quercetin (AuNPs-Qu-5) was synthesized and thoroughly characterized by several physicochemical techniques. AuNPs-Qu-5 showed nearly monodispersed spherical nanoparticles with average size of ~5.2 nm, whereas in free gold nanoparticles, average size was ~3.5 nm which was calculated from size distribution plot. FT-IR studies, thus, proved that Qu was conjugated with AuNPs through the interaction between Au with polar –OH group of Qu. Anticancer activity was evaluated by several in vitro assays, through which the IC_{50} values of AuNPs-Qu-5 for MCF-7 and MDA-MB-231 were found to be 50 and 100 μM, respectively, and the free Qu IC_{50} values for MCF-7 and MDA-MB-231 were 100 and 125 μM, respectively. We also demonstrated that AuNPs-Qu-5 enhanced anticancer effect and consequent higher apoptosis in breast cancer cells (100 and 125 μM).[33] Hence, for further studies, the MCF-7 cells were treated with 50 μM AuNPs-Qu-5 and MDA-MB-231 with 100 μM of AuNPs-Qu-5.

Metastasis remains one of the most life-threatening pathological events that represent the dissemination of cancer cells from origin to anatomically distant organ sites progressively. Cell migration and invasion are also crucial steps that involve embryogenesis, angiogenesis, tumour progression and inflammation interplay in a complex scenario. E-cadherin acts as a tumour suppressor inhibiting invasion and metastasis, and it is frequently repressed during tumour progression. Previous reports suggest that E-cadherin expression is downregulated in poorly differentiated tumour cells, such as breast cancer,[7] stomach cancer[8] and liver cancer.[9] Our results exhibit that AuNPs-Qu-5 inhibited the migration and invasion of breast cancer cells. However, AuNPs-Qu-5 upregulated epithelial maker of E-cadherin expression and downregulated mesenchymal markers of N-cadherin and vimentin protein expression upon AuNPs-Qu-5 treatment. This implies reduced migratory and invasive property upon AuNPs-Qu-5 treatment, which is likely due to modulation of EMT-related protein expression.

Snail is known to mediate EMT *via* down-regulation of cell adhesion molecules, such as E-cadherin by binding several E-boxes located in the promoter region.[34] Present study shows that AuNPs-Qu-5 inhibits the transcriptional repressors Snail, Slug and Twist at translational level in MCF-7 and MDA-MB-231 cells. This may be a reason for up-regulation of E-cadherin and down-regulation of N-cadherin and vimentin protein expression by treatment with AuNPs-Qu-5 in both cancer cell lines. AuNPs-Qu-5 may inhibit the EMT at the translational level. Similarly, earlier study from our group Bhat et al. [20] also reported that quercetin reverses the EGF-induced EMT in prostate cancer cells.

Snail up-regulates matrix metalloproteinase-9 (MMP) which contributes to extracellular matrix (ECM) invasion. Matrix metalloproteinases (MMPs) degrade structural components of the ECM, which allows tumour invasion and metastasis. MMP-2 and MMP-9 plays an important role in the processes of invasive metastasis and angiogenesis in various tumours.[35] Present study indicated that AuNPs-Qu-5 inhibits the action of MMP-2 and MMP-9 in MCF-7 and MDA-MB-231 cells. Earlier study from our group Vijayababu et al.[36] has reported that Quercetin inhibits the action of MMP-2 and MMP-9 in PC-3 cells. In this study, AuNPs-Qu-5 inhibits the MMP-2 and MMP-9 protein levels in MCF-7 and MDA-MB-231 cells, which would impact EMT.

Growth factors and cytokines can promote EMT triggering-specific signalling networks, including EGF and vascular endothelial growth factor, which is up-regulated in cervical cancer.[37] EMT has also been characterized in epithelial cancers, where tumour cells undergo this transition to promote invasion, migration and subsequent metastasis.[38,39] During EMT, the elevated Snail along with MMP-2 and MMP-9 activates EGF receptors that constitutively get phosphorylated and subsequently activate PI3K/Akt signalling pathways.[40] VEGFR-2 plays a critical role in endothelial cells proliferation, migration and tube formation by activating the phosphorylation of various downstream signalling molecules such as phosphatidylinositide 3-kinase (PI3K/Akt) and p38 mitogen-activated protein kinase (p38MAPK) signalling pathways which are constitutively activated in many cancers including breast tumour growth.[13,41] To assess whether AuNPs-Qu-5 affects these signalling pathways, we analysed the protein expression of the implicated pathway components. It was found that AuNPs-Qu-5 inhibits VEGFR-2/p-EGFR protein expression as well as the downstream molecules of p-PI3K/Akt/p-GSK-3β at translational level in MCF-7 and MDA-MB-231 cells.

Endothelial cells are currently used as in vitro model system for various physiological and pathological processes, especially in angiogenesis studies. Various reports have shown that tumours promote the angiogenic process, including the proliferation and migration of endothelial cells. One novel strategy to suppress tumour development is the inhibition of angiogenesis.[13,42] This study revealed that AuNPs-Qu-5 inhibits the growth of HUVEC in a dose-dependent manner. In addition, AuNPs-Qu-5 inhibits migration and invasion of endothelial cells. Our results affirm that of Wu et al.[43] that quercetin (Qu)-loaded polymeric micelles nanoparticles (Que micelles) at 10 μg concentration significantly inhibited HUVEC proliferation, migration, invasion and tube formation.

Angiogenesis, the formation of new blood vessels from the preexisting vasculature, plays a vital role in physiological and pathological processes, such as wound healing, embryonic development, tumour growth and metastasis.[44,45] Endothelial cell lines can be used as an in vitro model for angiogenesis studies.[46] Angiogenesis is key of tumour growth and progression. In addition to our analyses on the impact of AuNPs-Qu-5 on EMT, we also investigated the effect of AuNPs-Qu-5 on angiogenesis in HUVECs. It was found that AuNPs-Qu-5 inhibits in vitro angiogenesis by suppressing the capillary-like tube formation assay in HUVECs.

Among angiogenesis assays, CEA assay is the well-established and widely used model to confirm ex vivo anti-angiogenesis effect.[28,47] We observed that AuNPs-Qu-5 inhibited neovascularization compared with free Qu. Our data are consistent with the earlier study by Zhao et al.,[48] which reported that quercetin inhibits HUVEC proliferation, tube formation and angiogenesis in larval zebrafish. VEGF regulates

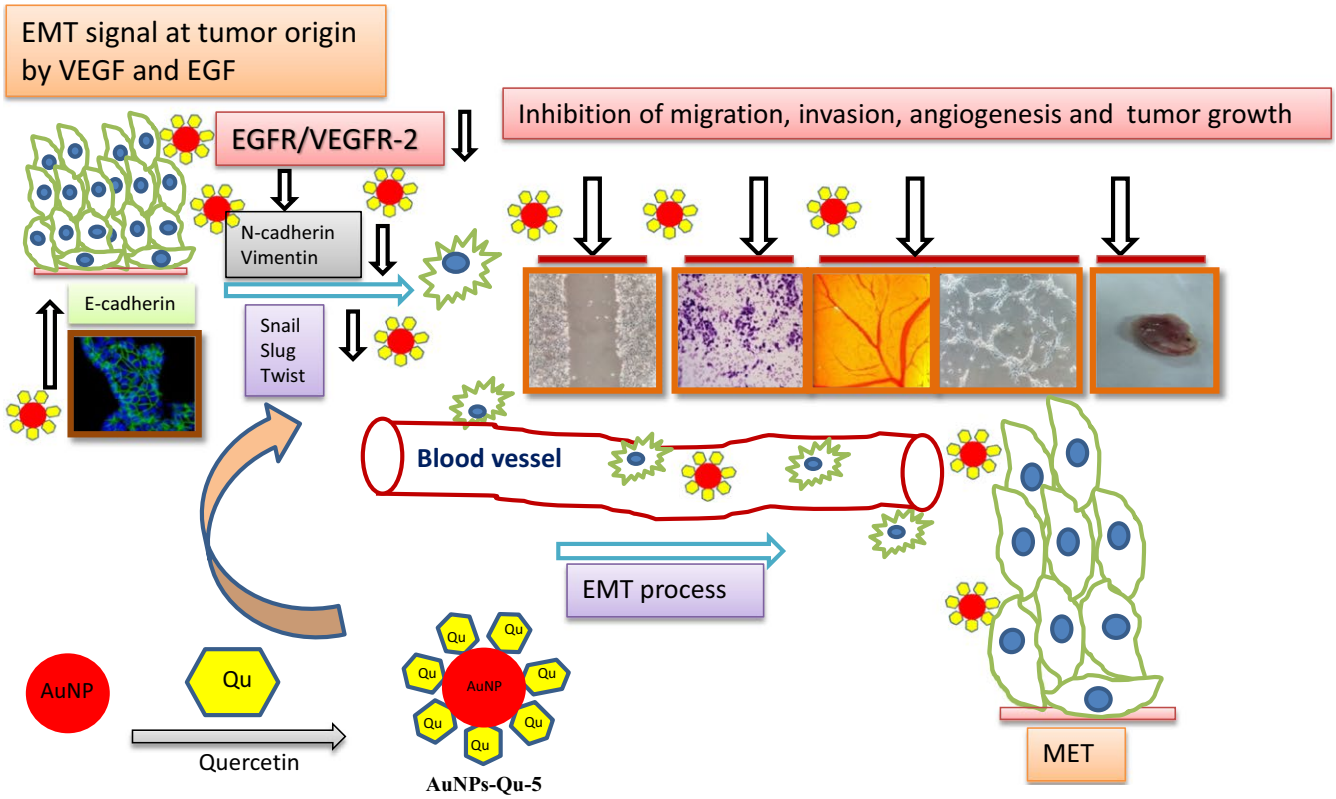

SCHEME 1 The overall schematic representation of the study throws light on the molecular level inhibition of AuNPs-Qu-5 on EMT, migration, invasion, angiogenesis and tumour growth

endothelial cell proliferation, migration, differentiation, tube formation and angiogenesis.[49] Our study shows that AuNPs-Qu-5 (50 μM) inhibits VEGFR-2 protein expression in HUVECs. Li et al.[50] also reported that quercetin inhibits the vascular endothelial growth factor-induced VEFGR-2 protein expression and downstream signal pathway in Rhesus macaque choroid-retinal endothelial cell line (RF/6A).

Given the inhibitory effect of AuNPs-Qu-5 on EMT as well as angiogenesis, we directly tested its anti-tumour efficacy. Towards this, we employed 7,12-dimethyl benz(a)anthracene (DMBA)-induced breast cancer in Sprague-Dawley rats.[29] After the tumour appearance, animals received AuNPs, free Qu and AuNPs-Qu-5 for 8 days. AuNP-treated tumour-bearing animals did not exhibit any anti-tumour activity, whereas the tumour volume or size reduced significantly for AuNPs-Qu-5-treated animals compared with those treated with free Qu. Remarkably, the AuNPs-Qu-5 treatment also prolonged the survival of tumour-bearing rats. Our results are in line with other studies where the antitumour effect of quercetin in vivo was reported.[51]

In a study conducted on mice subcutaneously xenografted with U937 cells, quercetin significantly diminished the tumour volume.[52] Quercetin displayed an inhibiting activity towards the invasiveness of the tumours and also decreased the volume of DMBA-induced mammary primary tumours in rats.[51] Histopathological examinations also proved that treatment with AuNPs-Qu-5 restorated epithelial mammary tissue architecture. Together our results show that AuNP conjugation enhanced the therapeutic effect of Qu in both in vitro and in vivo models, and this is the first report of its kind.

The overall schematic representation of the study throws light on the molecular level inhibition of AuNPs-Qu-5 on EMT, migration, invasion, angiogenesis and tumour growth (Scheme 1).

5 | CONCLUSION

This is the first report that reveals the anti-tumorigenic potential of gold nanoparticle–conjugated quercetin that inhibits EMT at molecular level. AuNPs-Qu-5 enhanced its anti-angiogenic activity of both in vitro (HUVECs) and ex vivo better than free Qu. Furthermore, AuNPs-Qu-5 decreased tumour burden in DMBA-induced mammary carcinoma in Sprague-Dawley rats. Histopathological examination also projects the protective role of AuNPs-Qu-5 by revitalizing the tumour cells to near normal. Hence, it is concluded that gold nanoparticles enhanced the therapeutic effect of quercetin; however, more in vivo studies are warranted to establish the clinical efficacy of these preparations.

ACKNOWLEDGEMENTS

SB is grateful to the University of Madras for University Research fellowship. CRP is grateful to CSIR, New Delhi, for generous financial support by the 12th Five Year Plan projects (Advanced Drug Delivery System: CSC0302 and SMiLE CSC0111). SM and SD are thankful to CSIR and UGC, New Delhi, for their respective research fellowship. The authors are thankful to Mass and Analytical Division, CSIR-IICT,

for performing ICPOES analysis (AARF project, CSIR 12th FYP) in detection of metal content in biological samples.

CONFLICTS OF INTEREST

None.

REFERENCES

1. American Cancer Society. *Cancer Facts & Figures 2016*. Atlanta: American Cancer Society; 2016.
2. Weigelt B, Peterse JL, van't Veer LJ. Breast cancer metastasis: markers and models. *Nat Rev Cancer*. 2005;5:591–602.
3. Kalluri R, Neilson EG. Epithelial-mesenchymal transition and its implications for fibrosis. *J Clin Invest*. 2003;112:1776–1784.
4. Kalluri R, Weinberg RA. The basics of epithelial-mesenchymal transition. *J Clin Invest*. 2009;119:1420–1428.
5. De Craene B, Berx G. Regulatory networks defining EMT during cancer initiation and progression. *Nat Rev Cancer*. 2013;13:97–110.
6. Van Roy F, Berx G. The cell-cell adhesion molecule E-cadherin. *Cell Mol Life Sci*. 2008;65:3756–3788.
7. Lai YJ, Tai CJ, Wang CW, et al. Anti-cancer activity of *Solanum nigrum* (AESN) through suppression of mitochondrial function and epithelial-mesenchymal transition (EMT) in breast cancer cells. *Molecules*. 2016;21:553.
8. Liu S, Chen D, Shen W, et al. EZH2 mediates the regulation of S100A4 on E-cadherin expression and the proliferation, migration of gastric cancer cells. *Hepatogastroenterology*. 2015;62:737–741.
9. Yang HD, Kim PJ, Eun JW, et al. Oncogenic potential of histone-variant H2A.Z.1 and its regulatory role in cell cycle and epithelial-mesenchymal transition in liver cancer. *Oncotarget*. 2016;7:11412–11423.
10. Bolós V, Peinado H, Pérez-Moreno MA, Fraga MF, Esteller M, Cano A. The transcription factor Slug represses E-cadherin expression and induces epithelial to mesenchymal transitions: a comparison with Snail and E47 repressors. *J Cell Sci*. 2003;116:499–511.
11. Hajra KM, Chen DY, Fearon ER. The SLUG zinc-finger protein represses E-cadherin in breast cancer. *Cancer Res*. 2002;62:1613–1618.
12. Li Y, Klausen C, Zhu H, Leung PC. Activin A increases human trophoblast invasion by inducing SNAIL-mediated MMP2 up-regulation through ALK4. *J Clin Endocrinol Metab*. 2015;100:1415–1427.
13. Pratheeshkumar P, Budhraja A, Son YO, et al. Quercetin inhibits angiogenesis mediated human prostate tumor growth by targeting VEGFR- 2 regulated AKT/mTOR/P70S6K signaling pathways. *PLoS ONE*. 2012;7:e47516.
14. Chen J, Wang T, Zhou YC, et al. Aquaporin 3 promotes epithelial-mesenchymal transition in gastric cancer. *J Exp Clin Cancer Res*. 2014;3:33–38.
15. Li L, Han R, Xiao H, et al. Metformin sensitizes EGFR-TKI-resistant human lung cancer cells in vitro and in vivo through inhibition of IL-6 signaling and EMT reversal. *Clin Cancer Res*. 2014;20:2714–2726.
16. Davis FM, Peters AA, Grice DM, et al. Non-stimulated, agonist-stimulated and store-operated Ca 2+ influx in MDA-MB-468 breast cancer cells and the effect of EGF-induced EMT on calcium entry. *PLoS ONE*. 2012;7:e36923.
17. Prenzel N, Fischer OM, Streit S, Hart S, Ullrich A. The epidermal growth factor receptor family as a central element for cellular signal transduction and diversification. *Endocr Relat Cancer*. 2001;8:11–31.
18. Androutsopoulos VP, Papakyriakou A, Vourloumis D, Tsatsakis AM, Spandidos DA. Dietary flavonoids in cancer therapy and prevention: substrates and inhibitors of cytochrome P450 CYP1 enzymes. *Pharmacol Ther*. 2010;126:9–20.
19. Liu HL, Jiang WB, Xie MX. Flavonoids: recent advances as anticancer drug. *Recent Pat Anticancer Drug Discov*. 2010;5:152–164.
20. Bhat FA, Sharmila G, Balakrishnan S, et al. Quercetin reverses EGF-induced epithelial to mesenchymal transition and invasiveness in prostate cancer (PC-3) cell line via EGFR/PI3K/Akt pathway. *J Nutr Biochem*. 2014;25:1132–1139.
21. Jain PK, Huang X, El-Sayed IH, El-Sayed MA. Noble metals on the nanoscale: optical and photothermal properties and some applications in imaging, sensing, biology, and medicine. *Acc Chem Res*. 2008;41:1578–1586.
22. Arshad A, Pandurangan A, Namrata S, Preeti A. A mini review on chemistry and biology of Hamelia Patens (Rubiaceae). *Pharmacogn J*. 2012;4:1–4.
23. Bhattacharya R, Mukherjee P, Xiong Z, Atala A, Soker S, Mukhopadhyay D. Gold nanoparticles inhibit VEGF165-induced proliferation of HUVEC cells. *Nano Lett*. 2004;4:2479–2481.
24. Mukherjee S, Chowdhury D, Kotcherlakota R, et al. Potential theranostics application of bio-synthesized silver nanoparticles (4-in-1 system). *Theranostics*. 2014;4:316–335.
25. Lowry OH, Rosebrough NJ, Farr AL, Randall RJ. Protein measurement with the Folin phenol reagent. *J Biol Chem*. 1951;193:265–275.
26. Mosmann T. Rapid colorimetric assay for cellular growth and survival: application to proliferation and cytotoxicity assays. *J Immunol Methods*. 1983;65:55–63.
27. Mukherjee S, Sriram P, Barui AK, et al. Graphene oxides show angiogenic properties. *Adv Healthc Mater*. 2015;4:1722–1732.
28. Barui AK, Veeriah V, Mukherjee S, et al. Zinc oxide nanoflowers make new blood vessels. *Nanoscale*. 2012;4:7861–7869.
29. Barros AC, Muranaka EN, Mori LJ, et al. Induction of experimental mammary carcinogenesis in rats with 7,12-dimethylbenz(a)anthracene. *Rev Hosp Clin Fac Med Sao Paulo*. 2004;59:257–261.
30. Bellamy LJ. *The Infrared Spectra of Complex Molecules*, 3rd ed. London: Chapman and Hall; 1975.
31. Sri KV, Kondaiah A, Ratna JV, Annapurna A. Preparation and characterization of quercetin and rutin cyclodextrin inclusion complexes. *Drug Dev Ind Pharm*. 2007;33:245–253.
32. Madhusudhan A, Reddy GB, Venkatesham M, et al. Efficient pH dependent drug delivery to target cancer cells by gold nanoparticles capped with carboxymethyl chitosan. *Int J Mol Sci*. 2014;15:8216–8234.
33. Balakrishnan S, Mukherjee S, Das S, Bhat FA, Patra CR, Arunakaran J. Abstract-NANOS 2015, International conference on Nanoscience, nanotechnology and advanced materials, 2015, GITAM University, Vishakapatnam, India. *P-Bio-*. 2015;101:p130.
34. Cano A, Pérez-Moreno MA, Rodrigo I, et al. The transcription factor snail controls epithelial-mesenchymal transitions by repressing E-cadherin expression. *Nat Cell Biol*. 2000;2:76–83.
35. Saarialho-Kere UK, Pentland AP, Birkedal-Hansen H, Parks WC, Welgus HG. Distinct populations of basal keratinocytes express stromelysin-1 and stromelysin-2 in chronic wounds. *J Clin Invest*. 1994;94:79–88.
36. Vijayababu MR, Arunkumar A, Kanagaraj P, Venkataraman P, Krishnamoorthy G, Arunakaran J. Quercetin downregulates matrix metalloproteinases 2 and 9 proteins expression in prostate cancer cells (PC-3). *Mol Cell Biochem*. 2006;287:109–116.
37. Mathur RS, Mathur SP. Vascular endothelial growth factor (VEGF) upregulates epidermal growth factor receptor (EGF-R) in cervical cancer *in vitro*: this action is mediated through HPV-E6 in HPV-positive cancers. *Gynecol Oncol*. 2005;97:206–213.
38. Boyer B, Vallés AM, Edme N. Induction and regulation of epithelial-mesenchymal transitions. *Biochem Pharmacol*. 2000;60:1091–1099.
39. Thiery JP. Epithelial-mesenchymal transitions in tumour progression. *Nat Rev Cancer*. 2002;2:442–454.
40. Lue HW, Yang X, Wang R, et al. LIV-1 promotes prostate cancer epithelial-to-mesenchymal transition and metastasis through

HB-EGF shedding and EGFR-mediated ERK signaling. *PLoS ONE*. 2011;6:27720.
41. Ferrara N, Frantz G, LeCouter J, et al. Differential expression of the angiogenic factor genes vascular endothelial growth factor (VEGF) and endocrine gland-derived VEGF in normal and polycystic human ovaries. *Am J Pathol*. 2003;162:1881–1893.
42. McMahon G. VEGF receptor signaling in tumor angiogenesis. *Oncologist*. 2000;5:3–10.
43. Wu Q, Deng S, Li L, et al. Biodegradable polymeric micelle-encapsulated quercetin suppresses tumor growth and metastasis in both transgenic zebrafish and mouse models. *Nanoscale*. 2013;5:12480–12493.
44. Hillen F, Griffioen AW. Tumour vascularization: sprouting angiogenesis and beyond. *Cancer Metastasis Rev*. 2007;26:489–502.
45. Carmeliet P, Jain RK. Molecular mechanisms and clinical applications of angiogenesis. *Nature*. 2011;473:298–307.
46. Chen H, Campbell RA, Chang Y, et al. Pleiotrophin produced by multiple myeloma induces transdifferentiation of monocytes into vascular endothelial cells: a novel mechanism of tumor-induced vasculogenesis. *Blood*. 2009;113:1992–2002.
47. Tufan AC, Satiroglu-Tufan NL. The chick embryo chorioallantoic membrane as a model system for the study of tumor angiogenesis, invasion and development of anti-angiogenic agents. *Curr Cancer Drug Targets*. 2005;5:249–266.
48. Zhao D, Qin C, Fan X, Li Y, Gu B. Inhibitory effects of quercetin on angiogenesis in larval zebrafish and human umbilical vein endothelial cells. *Eur J Pharmacol*. 2014;723:360–367.
49. Nakatsu MN, Sainson RC, Pérez-del-Pulgar S, et al. VEGF (121) and VEGF(165) regulate blood vessel diameter through vascular endothelial growth factor receptor 2 in an *in vitro* angiogenesis model. *Lab Invest*. 2003;83:1873–1885.
50. Li F, Bai Y, Zhao M, et al. Quercetin inhibits vascular endothelial growth factor-induced choroidal and retinal angiogenesis *in vitro*. *Ophthalmic Res*. 2015;53:109–116.
51. Devipriya S, Ganapathy V, Shyamaladevi CS. Suppression of tumor growth and invasion in 9,10 dimethyl benz(a) anthracene induced mammary carcinoma by the plant bioflavonoid quercetin. *Chem Biol Interact*. 2006;162:106–113.
52. Cheng S, Gao N, Zhang Z, et al. Quercetin induces tumor-selective apoptosis through downregulation of Mcl-1 and activation of Bax. *Clin Cancer Res*. 2010;16:5679–5691.

SUPPORTING INFORMATION

Additional Supporting Information may be found online in the supporting information tab for this article.